Journal of Advanced Research 77 (2025) 585–603

Contents lists available at ScienceDirect

Journal of Advanced Research

journal homepage: www.elsevier.com/locate/jare

CDK8 mediated inflammatory microenvironment aggravates osteoarthritis progression

Zhongnan Lin [a,b,c,1], Yining Xu [a,b,c,1], Hongyi Jiang [a,b,c,1], Wen Zeng [d], Yuhan Wang [a,b,c], Liang Zhu [a,b,c], Chihao Lin [a,b,c], Chao Lou [a,b,c], Hanting Shen [a,b,c], Han Ye [e], Yean Gu [c], Huachen Yu [a,b,c], Xiaoyun Pan [a,b,c,*], Lin Zheng [a,b,c,*]

[a] Department of Orthopedics, The Second Affiliated Hospital and Yuying Children's Hospital of Wenzhou Medical University Wenzhou Zhejiang Province China
[b] Key Laboratory of Orthopedics of Zhejiang Province Wenzhou Zhejiang Province China
[c] The Second Clinical School of Medicine Wenzhou Medical University Wenzhou Zhejiang Province China
[d] Experiemtial Center of Basic Medicine, School of Basic Medical Sciences Wenzhou Medical University Wenzhou China
[e] The Stomatology Hospital, Zhejiang University School of Medicine, China

HIGHLIGHTS

- CDK8 exerts its role in the progression of OA by influencing the transcriptional regulation of SASP genes through NF-κB.
- The mechanism by which CDK8 affects transcriptional regulation is through its cooperative recruitment with NF-κB to the promoters of SASP genes, followed by the promotion of Rpb1 CTD elongation phosphorylation in the gene-specific context induced by NF-κB.
- The expression level of CDK8 can affect the nuclear translocation of p65.
- Our study shows that based on ELISA detection of synovial fluid, serum, and cell culture supernatants, the secretion level of SASP may be positively correlated with the progression of OA, providing potential biomarkers for determining the severity of OA.
- In the development of OA, CDK8 not only affects the degradation of chondrocytes themselves but also promotes the inflammatory joint microenvironment and osteoclast differentiation of macrophages by regulating the secretion of SASP from chondrocytes.

GRAPHICAL ABSTRACT

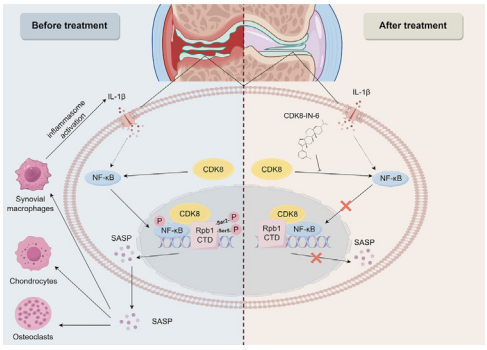

* Corresponding authors at: The Second Affiliated Hospital and Yuying Children's Hospital of Wenzhou Medical University Wenzhou, Zhejiang, China.
E-mail addresses: zjlinzhongnan@outlook.com (Z. Lin), xuyn@wmu.edu.cn (Y. Xu), jianghongyi0210@163.com (H. Jiang), 1371756448@qq.com (W. Zeng), 794171739@qq.com (Y. Wang), zila2000@163.com (L. Zhu), lch.1998@qq.com (C. Lin), lcjy0929@163.com (C. Lou), wanninghalo@163.com (H. Shen), 22418878@zju.edu.cn (H. Ye), wmugya@outlook.com (Y. Gu), huachenyu@126.com (H. Yu), xiaoyunpan@126.com (X. Pan), wzzl92@163.com (L. Zheng).
[1] These authors contributed equally to this work and share first authorship.

https://doi.org/10.1016/j.jare.2025.01.017
2090-1232/

ARTICLE INFO

Article history:
Received 7 November 2024
Revised 30 December 2024
Accepted 11 January 2025
Available online 12 January 2025

Keywords:
CDK8
Osteoarthritis
NF-κB
Transcriptional regulation
Transcriptional elongation

ABSTRACT

Introduction: Cyclin-Dependent Kinase 8 (CDK8), a CDK family member, regulates the development of inflammatory processes through transcriptional activation. The involvement of CDK8 in osteoarthritis (OA) progression is not yet understood.
Objectives: This study aims to investigate whether CDK8, through its transcriptional regulatory functions, collaborates with NF-κB in chondrocytes to regulate the transcription of senescence-associated secretory phenotype (SASP) genes, thereby exacerbating the inflammatory microenvironment in the progression of osteoarthritis (OA), and to explore the specific mechanisms involved.
Methods: The effects of CDK8 silencing or overexpression will be assessed by measuring OA pathological markers through H&E staining, immunoblotting, Western blot, qRT-PCR, immunofluorescence and ELISA. The DMM surgery mouse model will be used as the OA model, and the PAM and Von Frey tests will be employed to measure the pain threshold in mice. Luciferase and ChIP assays will be conducted to explore the transcriptional regulation and elongation mechanisms of CDK8.
Result: CDK8 influences OA advancement by being recruited to the SASP promoter region in cooperation with NF-κB, leading to the elongation phosphorylation of Rpb1 CTD within the context of NF-κB-induced gene specificity, thereby regulating SASP transcription. The SASP secreted by chondrocytes during this process promotes the inflammatory microenvironment in the joint and drives macrophage differentiation into osteoclasts, further worsening the severity of osteoarthritis.
Conclusion: The SASP secreted by chondrocytes during the OA process plays a crucial role in worsening the severity of the disease. Inhibiting CDK8 expression can decrease its secretion by downregulating the transcription levels of SASP, which are co-regulated by CDK8 and NF-κB. This could offer a new target for osteoarthritis treatment.

Introduction

Osteoarthritis (OA) is a prevalent long-term joint condition, marked by the progressive breakdown of cartilage and subsequent inflammation of the synovium [1,2]. This process ultimately leads to cartilage erosion, osteophyte formation, and joint space narrowing [3,4]. The main indicators of OA are pain and limited movement of the joints. In severe cases, osteoarthritis can lead to substantial impairment and is a major contributor to disability in the elderly population [5]. Currently, aside from surgery, effective treatments for OA remain limited [6,7]. Thus, obtaining a more complete understanding of the underlying biological pathways involved in the onset and development of OA is vital for improving patient outcomes and developing more effective treatments.

The pathogenesis of OA is complex, with inflammation being considered one of the key factors driving cartilage degradation and disease progression [8,9]. In particular, the senescence-associated secretory phenotype (SASP)—a pro-inflammatory molecular secretion state induced by cellular senescence—plays a critical role in OA [10]. SASP consists of inflammatory cytokines, chemokines, and proteases, which promote cartilage degradation through local inflammatory responses [11,12]. The transcription factor NF-κB has been shown to be a key regulator in initiating and maintaining SASP [13]. Therefore, investigating molecular pathways related to NF-κB and SASP may provide new therapeutic strategies for alleviating inflammation in OA.

In recent years, the role of cyclin-dependent kinases (CDKs) in the pathology of osteoarthritis (OA) has garnered widespread attention. As a class of multifunctional enzymes, CDKs can play important roles in inflammatory diseases and tissue degeneration by participating in cell cycle regulation and transcriptional control. For instance, CDK1 has been reported to accelerate OA progression by regulating the glycolytic pathway and promoting metabolic alterations in chondrocytes [14]. CDK4 and CDK6 primarily function through cell cycle regulation, playing key roles in chondrocyte proliferation and differentiation [15]. Additionally, CDK9 facilitates the transcriptional elongation of inflammation-related genes by phosphorylating the C-terminal domain (CTD) of RNA polymerase II (RNA Pol II) [16]. These studies indicate that different CDK family members perform diverse functions during OA pathogenesis, providing significant insights into exploring the specific molecular mechanisms of CDKs. As a transcription-associated CDK, CDK8 has attracted particular attention for its role in transcription and inflammation regulation [17]. CDK8 regulates the transcription process of RNA polymerase II (RNA Pol II) by forming a CDK8-Cyclin C complex and interacting with the Mediator complex [18,19]. CDK8 not only influences the transition between transcription initiation and elongation by phosphorylating the C-terminal domain (CTD) of RNA Pol II but also regulates transcriptional pausing by interacting with pausing factors [19]. Previous studies have shown that CDK8 contributes to the development of inflammation in the digestive and respiratory systems by enhancing the transcriptional activity of NF-κB [17,20]. However, whether CDK8 plays a role in the progression of OA through similar mechanisms remains unclear. Notably, in addition to the NF-κB signaling pathway, CDK8 also plays a significant role in other pathways closely associated with OA progression. Studies have shown that CDK8 influences the formation and degradation of the extracellular matrix (ECM) through the regulation of transcriptional enhancer acetylation, and the dynamic changes of the ECM are a core characteristic of OA development [21]. Furthermore, under mechanical stress, CDK8 is involved in the pathological processes of OA by regulating the expression of downstream factor mRNA levels [22]. Mechanical stress is not only a critical trigger for OA onset but also accelerates disease progression by regulating chondrocyte apoptosis and catabolic processes. These findings suggest that CDK8 may contribute to the pathophysiological processes of OA through multiple mechanisms, and its multifunctionality in transcriptional regulation makes it a potential breakthrough point for studying the mechanisms of OA pathogenesis.

Based on the above background, we hypothesize that CDK8 may play a critical role in OA progression by enhancing the transcriptional activity of NF-κB, initiating and sustaining SASP, as well as regulating the dynamic balance of the extracellular matrix and the transcriptional mechanisms responding to mechanical stress. This study aims to elucidate the specific molecular mechanisms of CDK8 in OA and evaluate its feasibility as a potential therapeutic target for OA. Notably, the development of CDK8 inhibitors has

shown significant therapeutic potential in other inflammatory diseases and cancer research in recent years [17,20]. Given the pivotal role of CDK8 in the regulation of inflammation and pathological processes in OA, our findings may provide important theoretical evidence and practical guidance for the development of specific CDK8 inhibitors to mitigate OA progression. This not only offers a novel perspective for existing OA treatment strategies but also has the potential to shift OA therapy from symptomatic management toward precise intervention.

Materials and methods

Ethics statement

The research involving human participants were reviewed and approved by Ethics Committee of the Second Affiliated Hospital of Wenzhou Medical University. The animal study was reviewed and approved by Wenzhou Medical University Animal Care and Use Committee.

Cell culture and treatment

All cells were cultured in a 37 °C incubator with 5 % CO_2. Human cartilage cell line C28/I2 (American Type Culture Collection (ATCC)), mouse macrophage cell line RAW 264.7 (ATCC), and mouse bone marrow-derived macrophages (BMDM) were all cultured using Dulbecco's Modified Eagle Medium (DMEM, Gibco, Invitrogen) supplemented with 10 % fetal bovine serum (FBS) and 1 % penicillin–streptomycin (Beyotime, China). Mouse primary chondrocytes were cultured in DMEM/F12 (Gibco, Invitrogen) supplemented with 10 % FBS and 1 % penicillin–streptomycin. Media were refreshed bi-daily, and passages were performed at 90 % cell confluence. At 50 % cell confluence, 10 ng/mL Interleukin (IL)-1β was introduced to C28/I2 or mouse primary chondrocytes to simulate the inflammatory conditions of osteoarthritis chondrocytes. Transfection was conducted at 50 % cell confluence. The supplementary table provides a list of the siRNA sequences used.

Quantitative Real-Time polymerase Chain Reaction (qPCR)

Using the spin column-based RNAeasy™ Animal RNA Extraction Kit extract RNA. The extracted RNA was reverse transcribed into cDNA and amplified. The $2-\Delta\Delta CT$ method was used to determine the relative gene expression level normalized to GAPDH. The supplementary table provides a list of the primers used.

CCK-8 assay

The cytotoxic effect of the CDK8 inhibitor CDK8-IN-6 (MCE, Cat. HY-147716) on C28/I2 cells and mouse chondrocytes was assessed using the Cell Counting Kit-8 (CCK-8, Elabscience). In serum-free medium, C28/I2 cells or mouse chondrocytes [8] were exposed to CDK8-IN-6 (0, 1, 2, 5, 10, or 20 μM) for 24 or 48 h. At the predetermined time points, add 10 μl of CCK-8 reagent to each well and then incubate for 2 h. Finally, the optical density (OD) was detected at 450 nm. All experiments were randomized and repeated independently in three separate experiments to ensure data reproducibility. Additionally, a blinded approach was used during data analysis to eliminate subjective bias.

Western blot

Using RIPA lysis buffer (Beyotime, China) to lyse Cells, and total protein content was measured with a bicinchoninic acid assay kit (Sigma, USA) before being denatured by boiling. Proteins (10 mg per well) were separated on SDS-PAGE gels and then transferred to PVDF membranes (Bio-Rad, USA). Membranes were blocked with 5 % skim milk for 2 h, followed by an overnight incubation at 4 °C with the primary antibody. Membranes were incubated with HRP-conjugated secondary antibody for 2 h following TBST washing. Subsequently detected using ECL reagent (Fudebio, China). Image Lab 3.0 software (Bio-Rad) was utilized to measure blot intensity. All Western Blot experiments were performed in three independent repetitions to ensure the reproducibility and statistical significance of the results. The primary antibodies used are listed as follows: Aggrecan (HuaBio, Cat. ET1704-57), COL2A1 (Abcam, Cat. ab34712), SOX9 (HuaBio, Cat. et1611-56), MMP3 (Abcam, Cat. ab52915), MMP13 (Abcam, Cat. ab39012), CDK8 (Proteintech, Cat. 22067–1-AP), p65 (CST, Cat. 8242), p-p65 (Affinity, Cat. AF2006), IκBα (CST, Cat. 4814), p-IκBα (CST, Cat. 2859), Rpb1 CTD (CST, Cat. 2629), p-Rpb1 CTD (ser 2) (CST, Cat. 13499), p-Rpb1 CTD (ser 5) (CST, Cat. 13523), Cleaved Caspase-1(CST, Cat. 89332), Cleaved-IL-1β (CST, Cat. 63124), Caspase1 (HuaBio, Cat. ET1608-69), NLRP3 (Abcam, Cat. ab214185), ASC (Proteintech, Cat. 10500–1-AP), FLAG (HuaBio, Cat. 0912–1), β-Actin (Fudebio, Cat. FD0060), Histone H3 (Proteintech, Cat. 68345–1-Ig), IgG (Proteintech, Cat. 30000–0-AP).

Immunofluorescence (IF)

Cells were fixed with 4 % paraformaldehyde and permeabilized using 0.5 % TritonX-100, each for 30 min. Blocking was performed for 1 h using a 10 % goat serum solution, followed by an overnight incubation with the primary antibody at 4 °C. Following PBS washes, the cells were incubated with Alexa Fluor 594 or Alexa Fluor 488-conjugated secondary antibodies (Beyotime, China) for 1 h. Nuclei were DAPI-stained. Fluorescence microscopy was employed to capture images. For the immunofluorescence experiments, cells from different regions were randomly selected for imaging, and the experiments were repeated three times. All sample processing and result acquisition were conducted by different researchers to implement blinding and minimize bias.

Histology and immunohistochemistry

Joint samples from mice were fixed in 4 % paraformaldehyde for 48 h after excising surrounding tissues. The joints were decalcified at 4 °C for one month using a shaker with a 10 % EDTA solution. The decalcified tissues underwent dehydration using a graded alcohol series before being embedded in paraffin. Using a microtome, the material was sectioned into 5-μm slices. Histological analysis employed Safranin O-fast green (S-O) and Hematoxylin-Eosin (H&E) staining for morphological evaluation and quantification, focusing on cartilage microstructure alterations and synovitis severity. The OARSI scoring system and synovitis scoring were used for semi-quantitative analysis of OA progression and synovial inflammation status [23–25]. Sections for immunohistochemistry were deparaffinized using xylene and rehydrated with graded ethanol. The tissue sections were then treated with trypsin-EDTA solution (0.25 %) and 3 % hydrogen peroxide, after incubating with specific antibodies overnight, the sections were treated with horseradish peroxidase (HRP)-conjugated secondary antibodies, and staining was performed using 3,3′-diaminobenzidine (DAB) (Beyotime, China). The sections were counterstained with hematoxylin (Beyotime, China), and after washing the sections, they were scanned using the KEYENCE BZ-H4XD fluorescence microscopy imaging system. To ensure consistency in scoring, all tissue sections were analyzed and scored by independent researchers under blinded conditions.

DMM mouse model and drug administration.

Eight-week-old male mice underwent either destabilization of the medial meniscus (DMM) surgery or a sham operation. In the DMM surgery, general anesthesia was administered, and a 0.5 cm incision was made on the medial parapatellar region of the right hind knee. The soft tissue was bluntly separated to expose the knee joint cavity. The anterior medial meniscotibial ligament was then transected. After the ligament was transected, the skin and joint capsule were sutured individually. During the sham surgery, after the soft tissue was separated, the anterior medial meniscotibial ligament was preserved, and the skin and joint capsule were sutured individually. For the CDK8 overexpression group (OE CDK8), two days after the DMM surgery, 10 μl of lentivirus (LV-CDK8) was administered into the joint cavity. The same batch of DMM and sham group mice received an injection of 10 μl lentivirus (LV-NC). For the CDK8 silencing group (sh-CDK8), two days after DMM surgery, 10 μl of adeno-associated virus (AAV-sh-CDK8) was administered into the joint cavity. The same batch of DMM and sham group mice received an injection of 10 μl adeno-associated virus (AAV-sh-NC). The adeno-associated virus serotype AAV5 was selected for the experiment. For the drug treatment group, one week after DMM surgery, 10 μl of CDK8-IN-6 (5 mg/kg) dissolved in DMSO was administered into the joint cavity twice a week. Conversely, the same batch of DMM and sham group mice received an injection of DMSO as a control. All injections were performed by the same individual. To minimize experimental bias, mouse grouping and surgeries were conducted using randomization methods, and the subsequent injection process was performed in a blinded manner. Eight weeks after the DMM surgery, the mice were euthanized, and knee joint samples were collected. The supplementary table provides a list of the shRNA sequences used.

Behavioral assessment

Pressure Application Measurement (PAM, Ugo Basile, Cat.38500) test and Von Fery (Aesthesio, USA, Cat.514000-20C) test were used to evaluate the pain of mice. In the PAM test, mice were gently restrained by hand, and their hind paws were lightly pinned to maintain consistent flexion at a similar angle for each mouse. The PAM transducer was applied with pressure to the medial side of the knee. The force exerted when the mice attempted to withdraw their knee was recorded. For Von Frey test, the mice were restrained in the same manner as described above. We then began pricking the inside of the knee with a 1.0 g filament. If the mice attempted to withdraw their knee, it was recorded as a positive response. We used the up-down method to calculate the withdrawal threshold [26]. Both tests were conducted before surgery and at 1, 2, 4, 6, and 8 weeks after DMM surgery. All behavioral assessments were conducted on randomly selected mice, and the experimenters were blinded to the grouping information to avoid subjective bias.

RNA sequencing

RNA sequencing was performed by Oebiotech (Shanghai, China). Briefly, C28/I2 cells were grouped and transfected with si-CDK8 or si-NC, then treated with or without IL-1β for 48 h before being sent to the technical provider, with three replicates per group. GO analysis was employed to interpret the biological significance of differentially expressed genes. Pathway analysis was based on the KEGG database to determine the pathways significantly affected by differentially expressed genes.

Senescence-associated β-galactosidase (SA-β-Gal)

SA-β-Gal staining was conducted using SA-β-Gal staining kit (Beyotime, China) following the provided instructions. After rinsing the stain with PBS, the blue staining of the cells was observed under a × 10 magnification microscope. All staining experiments were repeated three times, and different fields of view were randomly captured to obtain representative images.

Drug Affinity Responsive target Stability (DARTS)

The DARTS assay is used to screen for proteins that can bind to small molecule drugs. It operates on the principle that when a small molecule drug binds to its target proteins, it decreases the proteins' sensitivity to proteases. Proteins were exposed to CDK8-IN-6 at concentrations of 0.5, 1, 2, and 5 μM, or to DMSO, for 1 h. They were then digested with 1 μg/ml Pronase E (MCE, Cat.HY-114158) for 10 min, then proteolysis was inhibited with phenylmethylsulfonyl fluoride (PMSF) on ice for 5 min. Target protein levels were evaluated using Western blot analysis.

Co-immunoprecipitation assay

After lysing the cells using cold IP lysis buffer (Servicebio, China), the cells were sonicated. The processed lysis buffer was centrifuged at 12,000 rpm for 10 min at 4 °C to collect the supernatant. A specific antibody was added to the lysis buffer and incubated overnight at 4 °C. After washing the protein A/G magnetic beads with PBS, they were incubated with the cell lysis buffer containing the specific antibody for 1 h. The magnetic beads were washed and mixed thoroughly with 1 × loading buffer, then heated at 95 °C for 5 min to elute the proteins. The eluted proteins were detected by Western blot.

Micromass culture and DMMB assay of GAG for cells

Micromass culture has been employed in prior research [27,28], to assess chondrogenesis and extracellular matrix deposition. Around 100,000 cells were seeded in the center of a 24-well plate and cultured for 7 days, with the medium changed every two days. The cells were fixed using 4 % paraformaldehyde and stained with either Safranin O (Solarbio, China) or Toluidine Blue (Solarbio, China). Glycosaminoglycans (GAG) were used to quantify cartilage degradation [29]. We determined the GAG content using the dimethylmethylene blue (DMMB) colorimetric assay. The medium from the last two days of culture in each well plate was collected and used to quantify the GAG released by the cells using the dye DMMB (Polysciences, USA). Chondroitin-6-sulfate sodium salt (Sigma, USA) was used as the standard control. The absorbance of each group was read at 520 nm to determine the amount of GAG in the medium.

Chromatin immunoprecipitation (ChIP) assay and ChIP-qPCR

ChIP assays were conducted following the manufacturer's protocol (Cell Signaling Technology, USA). In summary, approximately 5 million cells were exposed to 1 % formaldehyde to crosslink proteins with DNA. Chromatin was isolated, fragmented by sonication, and subjected to immunoprecipitation using the specified antibodies. The recovered DNA was analyzed by qPCR, and the supplementary table provides a list of the primers used. All ChIP experiments were repeated three times, and the amount of recovered DNA was measured using NanoDrop to verify the extraction quality.

Nucleic acid electrophoresis

The PCR-amplified DNA was examined via 2 % agarose gel electrophoresis using TAE buffer. Electrophoresis was conducted at 120 V for 30 min to separate the DNA. The bands were visualized under UV light.

Luciferase reporter assay

The reporter plasmids (containing sequences of IL-6, IL-8, MMP-13, or their truncated sequences, respectively) were constructed using pGL3-Firefly_Luciferase-Renilla_Luciferase. C28/I2 cells were seeded in 24-well plates and transfected when they reached 30 % confluence. The cells were co-transfected with plasmids containing the reporter gene using Lipofectamine 3000 reagent (Thermo, Cat. L3000001). After 48 h, a dual-luciferase reporter assay kit (Beyotime, China) was used to assess the activities of firefly luciferase (LUC) and Renilla luciferase (RLUC). LUC activity was normalized to RLUC activity to determine the ratio, and fold changes were calculated by comparing the ratios of each group to the control group. The luciferase assays were repeated three times, and the transfection efficiency of the reporter gene in each experimental group was validated using parallel samples. Statistical analysis was performed using one-way ANOVA, with the significance level set at $p < 0.05$. The experimental results were evaluated in a blinded manner by independent researchers.

Cell co-culture

Primary mouse chondrocytes at first passage were cultured in 10 cm dishes until reaching 50 % confluence and divided into four groups. Each group of cells was transfected with siRNA-NC, siRNA-CDK8 using Lipofectamine 3000 reagent (Thermo, Cat. L3000001), or with CDK8 lentivirus (LV-CDK8) or its control (LV-NC). After 24 h of culture, the cells were washed and then continued to be cultured in complete medium containing 10 ng/ml IL-1β. After 48 h of culture, the medium was collected. The medium was centrifuged at 3,600 rpm for 5 min and filtered through a 0.2 μm filter to eliminate cell debris. The conditioned medium (CM) was concentrated about 50 times using Amicon Ultra-15 centrifugal filters with a 10 kDa molecular weight limit (Millipore). The concentrated conditioned medium was stored at −80 °C until it was used for co-culture with other cells.

Cell migration assay

Serum-free DMEM (200 μl) containing 10,000 cells was added to the transwell (SAINING, Cat. 1102020-T) upper chamber. According to the grouping, conditional medium (300 μl) was added to the lower chamber. After 24 h, removed the cells in the upper chamber. Washing the bottom of the chamber with PBS, the cells were fixed with 4 % paraformaldehyde for 30 min. The cells were stained with 0.1 % crystal violet solution for 15 min and imaged using a microscope.

ELISA assay

Using commercial ELISA kits, the concentrations of target substances were measured in the culture supernatant, mouse serum, and human synovial fluid. The ELISA kits used are listed as follows: Human IL-8 ELISA Kit (Yeasen, Cat. 97035ES96), Mouse IL-6 ELISA Kit (Yeasen, Cat. 98027ES96), Human IL-6 ELISA Kit (Yeasen, Cat. 97068ES96), Mouse MMP-13 ELISA Kit (Elabscience, Cat. E-EL-M0076), Human MMP-13 ELISA Kit (Elabscience, Cat. E-EL-H6023), Mouse IL-1β ELISA Kit (Yeasen, Cat. 98024ES96). Each group of samples was tested in parallel three times, and statistical analysis of the experimental data was performed using Student's *t*-test, with the significance level set at $p < 0.05$.

Osteoclast generation and TRAP staining

BMDM cells (10,000 per well) were cultured in a 96-well plate with 50 ng/mL M−CSF and 100 ng/mL RANKL. The conditioned medium was added according to the grouping. After a 7-day culture period, the wells were rinsed, and TRAP-positive cells were identified using a TRAP staining kit (Biocat).

Microcomputed tomography (microCT)

The fixed knee joint samples were scanned using a microcomputed tomography (microCT) scanner (Skyscan1276, Bruker) with an isotropic voxel size of 6 μm. The scanning covered a 3 mm region of the distal femur and a 3 mm region of the proximal tibia. The scanning parameters were set to an effective pixel size of 8.82 μm, a current of 500 ÂμA, a voltage of 80 keV, with an exposure time of 1500 ms per 360 rotational steps. The image reconstruction and data analysis in microCT were performed by independent researchers in a blinded manner without knowledge of the experimental groupings. All scanning parameters were calibrated before each scan and repeated three times to ensure data accuracy and consistency.

Result

The overexpression of CDK8 exacerbates knee cartilage degeneration and pain in mice, as well as osteoarthritis in cells

To assess CDK8′s potential to induce OA in vivo, 10 μl of lentivirus (LV-CDK8) was administered into the joint cavity in the CDK8 overexpression group (OE CDK8) two days post-DMM surgery. Both the DMM and Sham group mice were administered an injection of 10 μl lentivirus (LV-NC). Eight weeks after surgery, histological analysis showed that the cartilage surface of the DMM group mice was incomplete, and matrix loss was observed. The CDK8 overexpression group showed a marked exacerbation of this phenomenon (Fig. 1A). The OARSI scores indicated that CDK8 overexpression further increased the severity of knee joint damage in mice after DMM surgery (Fig. 1B). Additionally, immunohistochemical staining confirmed a decrease in COL2A1 and aggrecan expression and an increase in MMP13 in cartilage exposed to CDK8 (Fig. 1C-F).

Chronic pain is a primary clinical symptom of OA. The Pressure Application Measurement (PAM) test and Von Frey filament test were used to measure the pain threshold in mice. Beginning in the fourth week, the DMM and CDK8 overexpression groups exhibited significantly lower pain thresholds compared to the Sham group. Moreover, compared to the DMM group, the CDK8 overexpression group exhibited even lower pain thresholds (Fig. 1G-H). To validate the effect of CDK8 overexpression on OA, C28/I2 cells were co-transfected with either pCMV-control or pCMV-CDK8 based on the grouping, followed by a 48-hour treatment with or without 10 ng/ml IL-1β.IL-1β stimulation markedly decreased aggrecan, COL2A1, and SOX9 levels in cells while increasing MMP-3 and MMP-13 expression. Additionally, these effects were further enhanced in cells overexpressing CDK8 (Fig. 1I and Fig. S1). Safranin O and Toluidine Blue staining were applied to C28/I2 cells and mouse chondrocytes to evaluate cartilage formation and degradation. Both cell types were co-transfected with either pCMV-CDK8 or pCMV-control and cultured in complete medium with 10 ng/ml IL-1β for 7 days. After overexpression of CDK8, cartilage formation significantly decreased (Fig. 1J), while

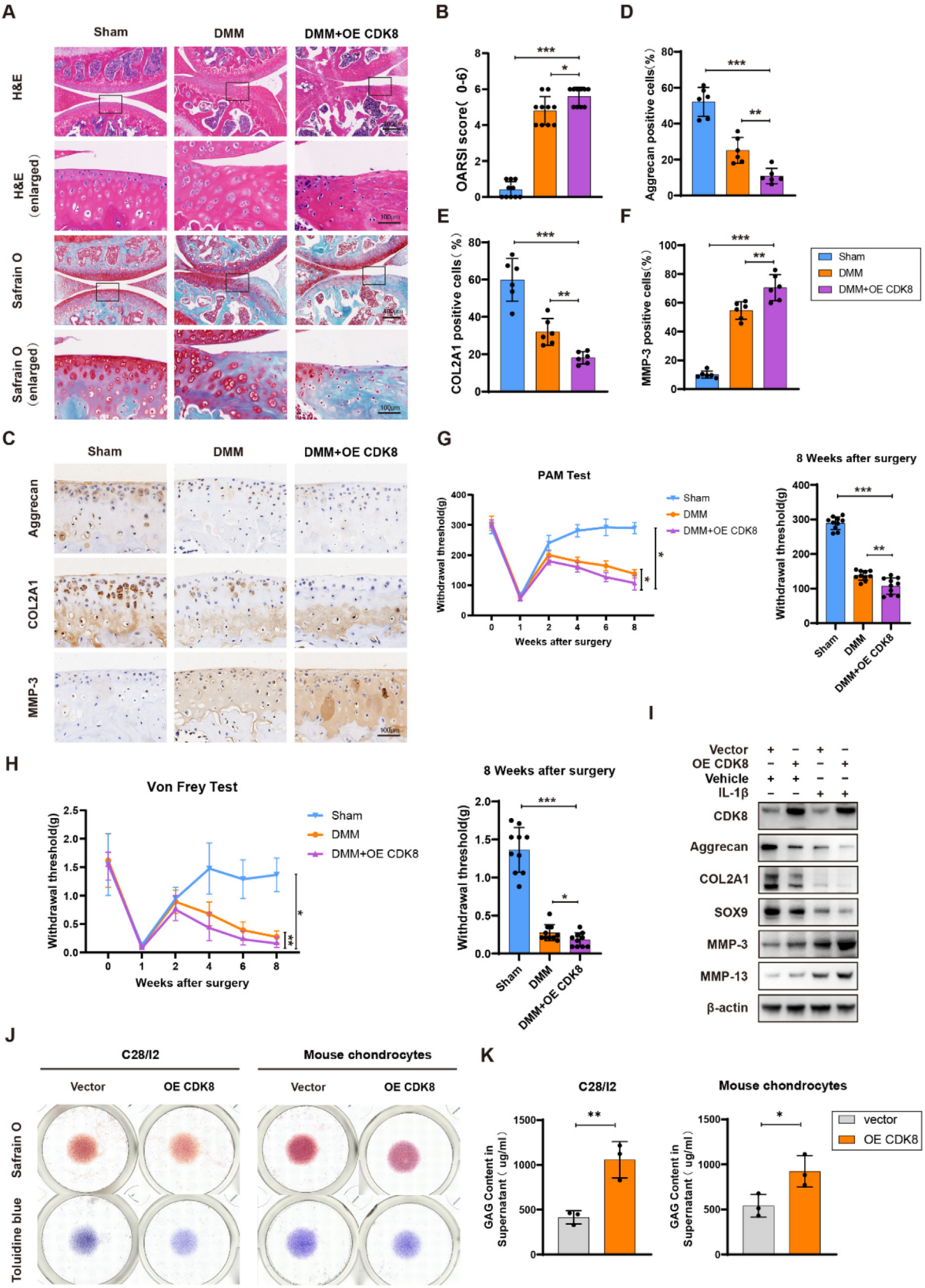
A
Sham
DMM
DMM+OE CDK8
H&E
H&E (enlarged)
Safrain O
Safrain O (enlarged)
B
OARSI score(0-6)
D
Aggrecan positive cells(%)
E
COL2A1 positive cells (%)
F
MMP-3 positive cells(%)
Sham
DMM
DMM+OE CDK8
C
Aggrecan
COL2A1
MMP-3
G
PAM Test
Withdrawal threshold(g)
Weeks after surgery
8 Weeks after surgery
H
Von Frey Test
I
Vector
OE CDK8
Vehicle
IL-1β
CDK8
Aggrecan
COL2A1
SOX9
MMP-3
MMP-13
β-actin
J
C28/I2
Mouse chondrocytes
Safrain O
Toluidine blue
K
GAG Content in Supernatant (ug/ml)
vector
OE CDK8

the GAG content resulting from cartilage degradation significantly increased (Fig. 1K). In summary, these data indicate that the overexpression of CDK8 exacerbates cartilage degradation and the progression of OA.

CDK8 knockdown alleviates knee cartilage degeneration and pain in mice and reduces osteoarthritis in cells

To elucidate CDK8′s role in chondrocyte inflammatory responses, CDK8-specific siRNA was transfected into C28/I2 cells and mouse chondrocytes. The efficiency of siRNA transfection was validated through Western blotting (Fig. S2A) and quantitatively assessed (Fig. S2B). Based on the knockdown efficiency of CDK8, we chose si-hCDK8#2 and si-mCDK8#1 for further experiments due to their effective CDK8 knockdown, transfecting them into C28/I2 cells and mouse chondrocytes, respectively.C28/I2 cells and mouse chondrocytes, with CDK8 knocked down, were exposed to IL-1β for 48 h.CDK8 knockdown restored the mRNA and protein levels of aggrecan, COL2A1, and SOX9, which were previously reduced by IL-1β stimulation, and decreased the levels of MMP-3 and MMP-13 (Fig. 2A-B and Fig. S2C-E). These results were further confirmed by immunofluorescence (IF) assays conducted in C28/I2 cells (Fig. 2C). Additionally, as shown by the results of Safranin O and Toluidine Blue staining, the decrease in cartilage formation induced by IL-1β stimulation was restored following co-treatment with si-CDK8 (Fig. 2D, E). Meanwhile, the GAG content resulting from cartilage degradation was correspondingly reduced (Fig. S2F, G). To investigate the in vivo effects of CDK8 knockdown, 10 μl of adenovirus (AAV-sh-CDK8) was administered into the joint cavity two days after DMM surgery in the CDK8 silencing group (sh-CDK8). The DMM group and Sham group mice received 10 μl of lentivirus (AAV-sh-NC) injections. Eight weeks after surgery, histological analysis showed that CDK8 knockdown rescued the cartilage degradation and matrix loss induced by DMM surgery in mice (Fig. 2F). The OARSI scores confirmed that CDK8 knockdown alleviated the severity of knee joint damage in mice post-DMM surgery (Fig. 2G). Additionally, results from the PAM test and Von Frey filament pain test indicated that CDK8 knockdown significantly reduced the degree of pain threshold reduction caused by DMM surgery in mice (Fig. 2H and Fig. S2H).

CDK8 is associated with senescence in chondrocytes and regulate their secretion of SASP

We conducted whole-transcriptome RNA sequencing on CDK8 knockout cell lines to explore the mechanisms by which CDK8 affects osteoarthritis progression and the associated signaling pathways. The volcano plot analysis identified 1,399 differentially expressed genes (DEGs) between CDK8 knockout cell lines and normal control C28/I2 cells, both treated with IL-1β. Among these, 803 were downregulated, including the SASP members IL-6, CXCL8 (IL-8), and MMP-13 (Fig. 3A). GO enrichment analysis of the DEGs revealed CDK8′s involvement in diverse cellular processes such as the cell cycle, cell division, and DNA replication regulation (Fig. S3A). KEGG enrichment analysis revealed a significant association of CDK8 with cellular senescence, NF-κB signaling, and cytokine-cytokine receptor interactions, as illustrated in Fig. 3B. Gene Set Enrichment Analysis (GSEA) validated CDK8′s role in chemokine signaling pathways and cytokine-cytokine receptor interaction (Fig. 3C-D).Comparable outcomes were noted in the GSEA analysis of differentially expressed genes between the Control and IL-1β treated groups (Fig. S3B-C).β-galactosidase assay was used to verify the impact of CDK8 on the progression of cellular senescence. After the second generation of mouse chondrocytes was transfected with si-CDK8 or si-NC according to the grouping, they were treated with *tert*-butyl hydroperoxide (t-BHP) for 24 h, followed by β-galactosidase staining. The results showed that CDK8 knockdown significantly suppressed the t-BHP-induced senescence progression in mouse chondrocytes (Fig. 3E).

The volcano plot results indicate a significant decrease in the expression of SASP members IL-6, IL-8, and MMP-13 following CDK8 knockdown. We conducted a retrospective study to determine if the levels of these three members were elevated in the synovial fluid of osteoarthritis (OA) patients. Eighty-seven OA patients were included based on the inclusion criteria and categorized into three stages using the Kellgren-Lawrence (KL) grading scale: mild (n = 23), moderate (n = 29), and severe (n = 35) (Fig. 3F).The levels of the three SASP members were notably elevated in the synovial fluid of OA patients compared to healthier individuals, with severe OA patients exhibiting significantly higher levels than those with moderate OA, indicating a potential positive correlation between SASP and OA progression (Fig. 3G). In mice, we conducted further validation. The ELISA results of mouse serum showed that CDK8 overexpression indeed led to an increase in SASP secretion in OA mice (since the IL-8 gene is absent in the mouse genome [30], this experiment only measured the levels of IL-6 and MMP-13) (Fig. 3H). In cells, we verified through qPCR experiments that the IL-1β-induced increase in SASP levels was reduced after CDK8 knockdown in C28/I2 cells and mouse chondrocytes (Fig. S3D). ELISA experiments showed similar results when C28/I2 cells and mouse chondrocytes with CDK8 knockdown were treated with IL-1β, TNF-α, and LPS, respectively (Fig. 3I). Therefore, we can confirm that CDK8 has a regulatory function on SASP.

CDK8 activates the NF-κB pathway and regulates the transcription of SASP

KEGG enrichment analysis indicates a close connection between CDK8 and the NF-κB signaling pathway. We found knocking down CDK8 significantly reduced the phosphorylation of IκBα and p65, while increasing total IκBα levels (Fig. 4A and Fig. S4A). Co-immunoprecipitation experiments further confirmed the inter-

Fig. 1. The overexpression of CDK8 exacerbates knee cartilage degeneration and pain in mice, as well as osteoarthritis in cells. (A) H&E and S-O staining of the knee joints in each group of mice 8 weeks after DMM surgery, (B) followed by assessment of OA severity in the mice using the OARSI scoring system. n = 10 per group. (C) Aggrecan, COL2A1, and MMP-3 expression were detected by immunohistochemical staining in the cartilage samples, (D-F) and quantitative analysis of the proportion of Aggrecan, COL2A1, and MMP-3 positive cells in each segment. n = 6 per group. (G-H) The Pressure Application Measurement (PAM) test and Von Frey filament test were used to assess the pain threshold in mice. (I) C28/I2 cells were transfected with pCMV-control or pCMV-CDK8 and then exposed to IL-1β for 48 h. Western blot analysis was performed to detect aggrecan, COL2A1, SOX9, MMP-3, and MMP-13. (J) C28/I2 and mouse chondrocytes were transfected with pCMV-CDK8 and treated with IL-1β for 7 days. Safranin O and Toluidine Blue staining were used to assess cartilage formation, (K) and the culture supernatants from the last two days were collected to analyze cartilage degradation using the DMMB method to measure GAG content. Data are presented as mean ± SD; *, $p < 0.05$; **, $p < 0.01$; ***, $p < 0.001$; ns, no significance; comparisons with the control group or as indicated. (For interpretation of the references to colour in this figure legend, the reader is referred to the web version of this article.)

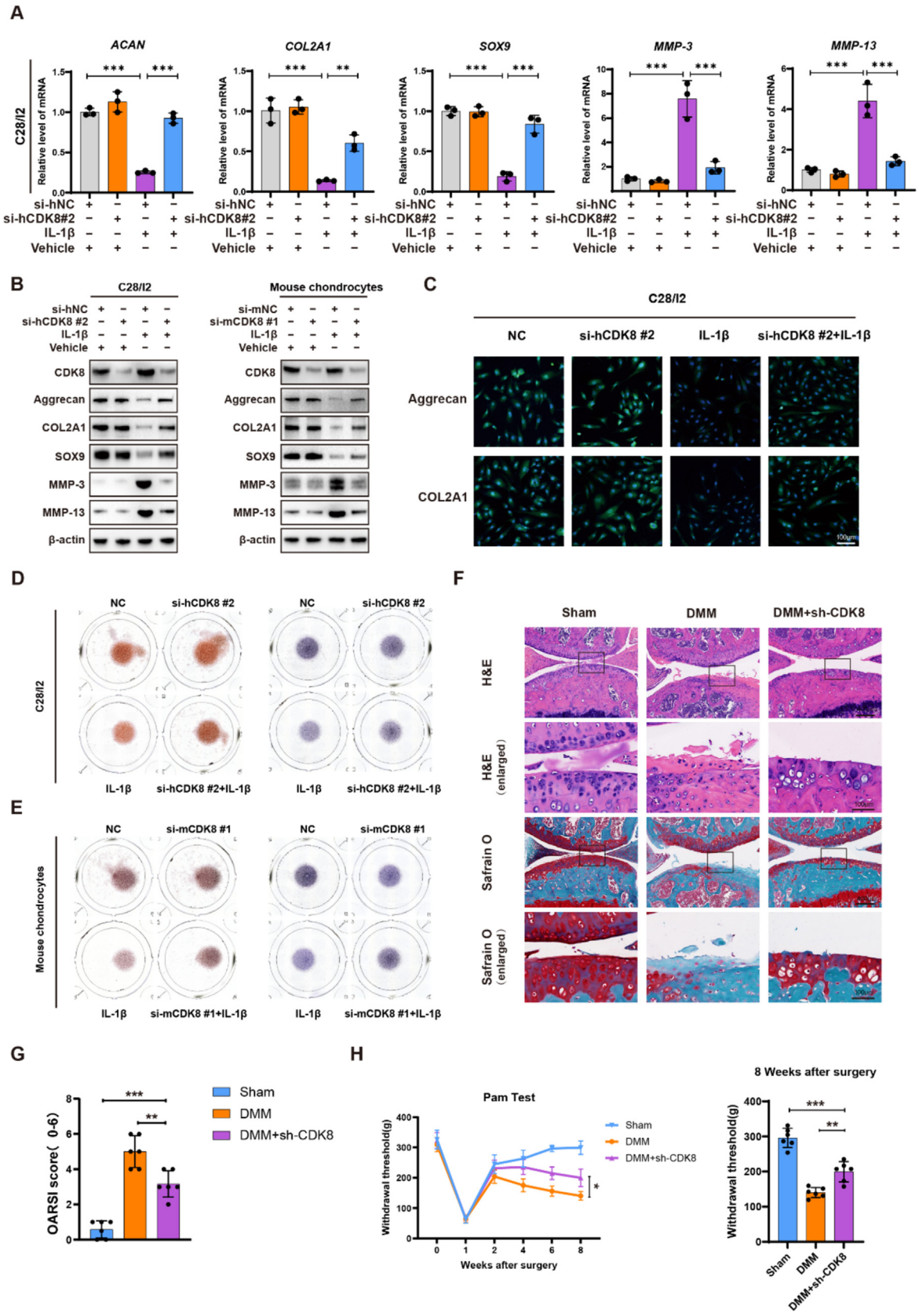
A
ACAN
COL2A1
SOX9
MMP-3
MMP-13
C28/I2
Relative level of mRNA
si-hNC
si-hCDK8#2
IL-1β
Vehicle
B
C28/I2
Mouse chondrocytes
si-hNC
si-hCDK8 #2
si-mNC
si-mCDK8 #1
CDK8
Aggrecan
COL2A1
SOX9
MMP-3
MMP-13
β-actin
C
C28/I2
NC
si-hCDK8 #2
IL-1β
si-hCDK8 #2+IL-1β
Aggrecan
COL2A1
D
NC
si-hCDK8 #2
C28/I2
IL-1β
si-hCDK8 #2+IL-1β
E
NC
si-mCDK8 #1
Mouse chondrocytes
IL-1β
si-mCDK8 #1+IL-1β
F
Sham
DMM
DMM+sh-CDK8
H&E
H&E (enlarged)
Safrain O
Safrain O (enlarged)
G
OARSI score(0-6)
Sham
DMM
DMM+sh-CDK8
H
Pam Test
Withdrawal threshold(g)
Weeks after surgery
8 Weeks after surgery

action between CDK8 and p65. CDK8-IN-6, an inhibitor of CDK8, was shown to weaken this interaction (Fig. 4B). Treatment with IL-1β significantly enhances the nuclear translocation of p65, resulting in increased colocalization of CDK8 and p65 in the nucleus (Fig. 4C). Conversely, knocking down CDK8 markedly reduces the nuclear translocation of p65 (Fig. S4B). The impact of CDK8 on p65 nuclear translocation can be further observed in the Western blot results (Fig. 4D). These findings confirm the close interaction between the transcription factor p65 and CDK8. To investigate how the interaction between CDK8 and p65 affects the content of SASP, we aimed to verify whether CDK8 regulates the transcription of SASP by influencing the function of p65 as a transcription factor. We identified the binding sequence of Vertebrata p65 on the JSAPAR website (Fig. S4C) and found the human IL-6, IL-8, and MMP-13 gene sequences on NCBI. There are p65 binding sites present in the promoter sequences of all three genes. The three pGL3 plasmids, each containing one of the three genes, were co-transfected into C28/I2 cells that had been transfected with either si-CDK8 or si-NC. Through a luciferase reporter assay, we confirmed that NF-κB can regulate the transcription of these three genes, and inhibiting CDK8 expression reduces the transcription levels of these NF-κB-regulated genes (Fig. 4E). To determine the position of the binding sites involved in NF-κB-regulated transcription in the promoters of these three genes, we listed the predicted p65 binding sites in the promoter sequences of these genes (Fig. S4D) and amplified several truncated fragments of the promoters from genomic DNA of C28/I2 cells to construct various luciferase reporter plasmids driven by different promoter regions. Based on the evaluation of the luciferase reporter assay, mutation of the predicted binding site 3 in the IL-6 promoter, and site 2 in the IL-8 and MMP promoters weakened the NF-κB-mediated enhancement of promoter reporter gene activity, indicating that these regions are direct binding sites for p65. (Fig. 4F). Using Chromatin immunoprecipitation (ChIP) assay, we further studied the effect of CDK8 on the binding of p65 to the SASP promoter regions in C28/I2 cells. According to the results of the luciferase reporter assay, we selected site 3 of the IL-6 gene and site 2 of the IL-8 and MMP-13 genes as the experimental sites. As shown by nucleic acid electrophoresis (Fig. 4G) and ChIP-qPCR analysis (Fig. 4H), knocking down CDK8 reduced the physical binding of p65 to the SASP gene promoter regions, while overexpressing CDK8 enhanced this effect.

CDK8 and NF-κB are cooperatively recruited to SASP promoters, leading to elongation phosphorylation of the Rpb1 CTD

To explore the precise mechanism through which CDK8 and NF-κB trigger SASP transcription, we analyzed the expression levels of the total RNA Pol II large subunit C-terminal domain (Rpb1 CTD) and its phosphorylated forms, Ser5 (promoting Pol II release from promoters) and Ser2 (allowing transcription elongation) [31,32], using western blot (Fig. S5A and B). We found that knocking down CDK8 inhibits IL-1β-induced phosphorylation of both forms of Rpb1 CTD. To further confirm this, in C28/I2 cells transfected with si-CDK8 or si-NC, we conducted a series of ChIP experiments after treatment with or without IL-1β. The ChIP analysis results for NF-κB-induced SASP members IL-6, IL-8, MMP-13, and the constitutively expressed housekeeping gene GAPDH are shown in Fig. 5. As anticipated, after IL-1β stimulation, the activated NF-κB p65 subunit binds to the promoter regions of SASP genes but not to the housekeeping genes. Knockdown of CDK8 reduces the binding of p65 to gene promoter regions (Fig. 5A). Additionally, CDK8 cooperatively recruits with p65 to the promoters and adjacent body regions of SASP genes but not to housekeeping genes. Knockdown of CDK8 similarly affects the IL-1β-induced recruitment of CDK8 (Fig. 5B). Subsequently, we examined the impact of IL-1β treatment and CDK8 knockdown on the binding of Rpb1 CTD (Fig. 5C), p-Rpb1 CTD (Ser5) (Fig. 5D), and p-Rpb1 CTD (Ser2) (Fig. 5E) to the promoters. IL-1β stimulated the binding of all three forms of Rpb1 CTD to the promoters and bodies of SASP genes, but did not stimulate their binding to housekeeping genes. Knocking down CDK8 strongly inhibits the binding of elongation-competent p-Rpb1 CTD (Ser2) to the gene bodies, with a weaker but still significant effect on total Rpb1 CTD and p-Rpb1 CTD (Ser5). This effect observed upon CDK8 depletion is pronounced for SASP genes but not observed for housekeeping genes. Therefore, we confirm that the specific mechanism by which CDK8 and NF-κB induce SASP transcription involves their cooperative recruitment to SASP promoters, followed by elongation phosphorylation of Rpb1 CTD in the gene-specific context induced by NF-κB.

CDK8 promotes the inflammatory microenvironment and osteoclast differentiation of macrophages by regulating the SASP in chondrocytes

Synovial macrophages are important immune cells in the synovial tissue, primarily located in the inner layer of the synovium. They are involved in the immune regulation and inflammatory response of the joint and play a key role in joint diseases, especially inflammatory diseases [33]. To investigate whether CDK8 influences the progression of OA by affecting synovial macrophages, we prepared conditional medium (CM) from the culture medium of mouse chondrocytes for the migration assay (Fig. 6A). To determine the appropriate concentration of CM, a CCK-8 assay was conducted. The results showed that at a 5-fold concentration, CM exhibited no cytotoxicity to RAW 264.7 cells and mouse BMDMs at 24 and 48 h (Fig. S6A). Therefore, this concentration of CM was used in all subsequent experiments. Additionally, we compared the SASP content between the supernatant of normal mouse chondrocytes and the 5-fold concentrated CM (Fig. S6B). According to the experimental groups, RAW 264.7 cells was cultured with CM for 48 h to perform the migration assay to assess the effect of CDK8 on the migration ability of mouse macrophages. The results showed that CDK8 knockdown reduced the migration ability of RAW 264.7 cells (Fig. 6B), whereas CDK8 overexpression had the opposite effect (Fig. 6C). Subsequently, BMDMs from mice were

Fig. 2. CDK8 knockdown alleviates knee cartilage degeneration and pain in mice and reduces osteoarthritis in cells. (A-B) C28/I2 cells and mouse chondrocytes were transfected with si-CDK8 or si-NC and then exposed to IL-1β for 48 h. (A) qRT-PCR and (B) Western blot analyses were used to detect the expression levels of aggrecan, COL2A1, SOX9, MMP-3, and MMP-13. (C) IF analysis was used to detect the expression of aggrecan and COL2A1 in C28/I2 cells transfected with si-CDK8 or si-NC and exposed to IL-1β for 48 h. (D, E) Safranin O and Toluidine Blue staining were used to assess cartilage formation, analyzed in (D) C28/I2 cells or (E) mouse chondrocytes, both transfected with si-CDK8 and treated with IL-1β for 7 days. (F) Hematoxylin and Eosin (H&E) staining and Safranin O/Fast Green staining of mouse knee joints 8 weeks after DMM surgery, and (G) the severity of osteoarthritis in mice was subsequently assessed using the OARSI scoring system. Each group, n = 6. (H) Pain threshold in mice was assessed using the pressure application measurement (PAM) test. Data are presented as mean ± SD; *, $p < 0.05$; **, $p < 0.01$; ***, $p < 0.001$; ns, no significance; comparisons with the control group or as indicated. (For interpretation of the references to colour in this figure legend, the reader is referred to the web version of this article.)

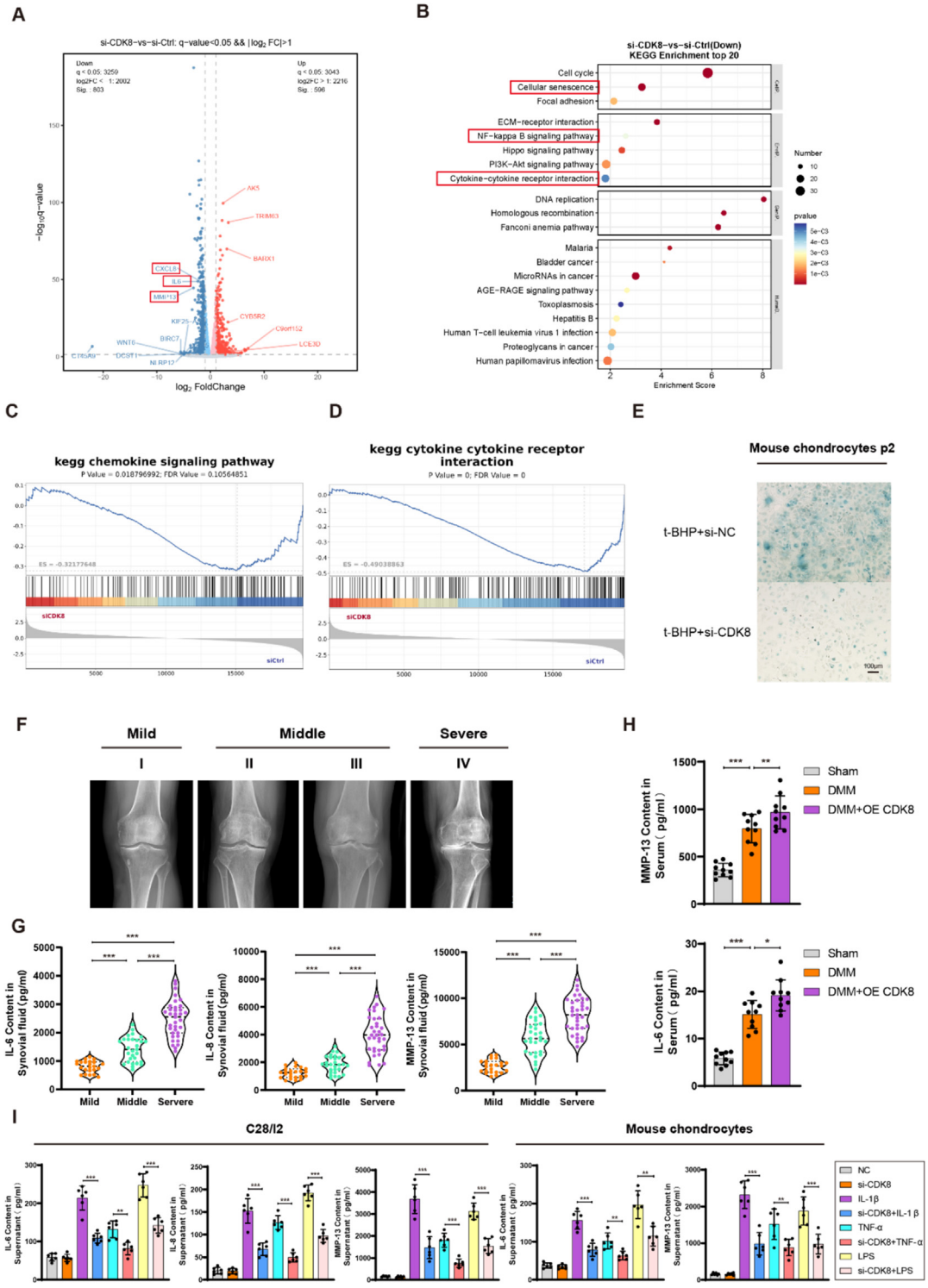

Fig. 3. CDK8 is associated with senescence in chondrocytes and regulate their secretion of SASP. (A) Volcano plot of differentially expressed genes from RNA sequencing data. (B) KEGG enrichment analysis of differentially expressed genes. (C-D) GSEA of differentially expressed genes. (E) β-galactosidase staining images of mouse chondrocytes with CDK8 knockdown, co-treated with t-BHP. (F) Representative knee X-rays of patients at different stages of osteoarthritis. According to the Kellgren-Lawrence (KL) grading of the tibiofemoral joint, patients were classified into four stages. Stage I is classified as mild osteoarthritis, n = 23; middle osteoarthritis included stages II and III, n = 29; and stage IV was defined as severe osteoarthritis, n = 35. (G-I) ELISA detection of SASP levels in (G) synovial fluid of patients with mild, moderate, and severe OA, (H) serum of mice, and (I) C28/I2 cells and mouse chondrocytes. Data are presented as mean ± SD; *, $p < 0.05$; **, $p < 0.01$; ***, $p < 0.001$; ns, no significance; comparisons with the control group or as indicated.

cultured with CM according to the grouping, and qPCR was used to analyze their M1 polarization markers. The study found that CDK8 knockdown inhibited M1 polarization markers such as iNOS, IL-1β, TNF-α, and CD86 in mouse BMDMs (Fig. S6C), whereas CDK8 overexpression increased the levels of these markers (Fig. S6D). Next, Western blot analysis was used to evaluate the impact of CDK8 on inflammasome activation in mouse BMDMs. As expected, CDK8 knockout inhibited inflammasome activation, reducing the

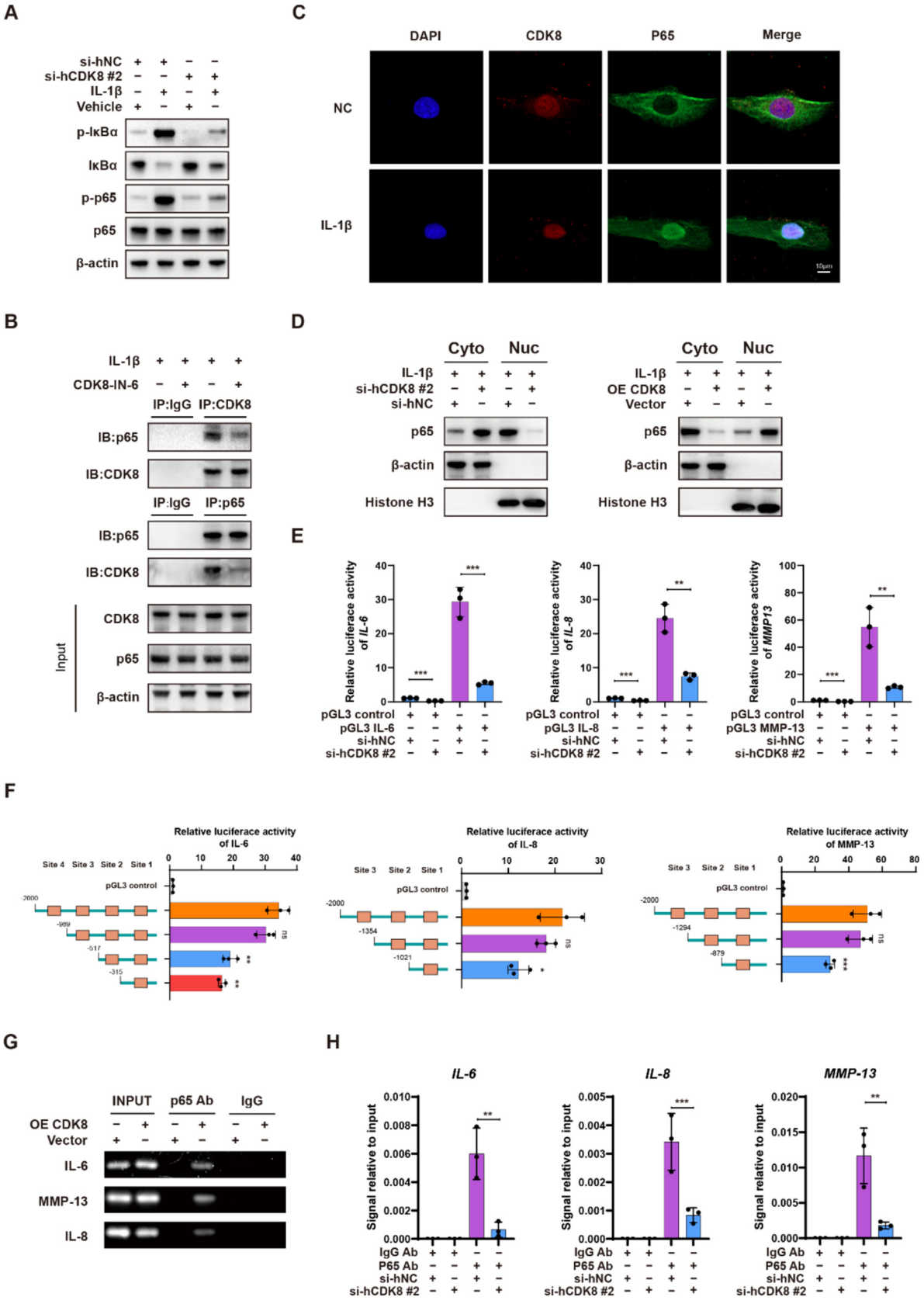
A
si-hNC
si-hCDK8 #2
IL-1β
Vehicle
p-IκBα
IκBα
p-p65
p65
β-actin
B
IL-1β
CDK8-IN-6
IP:IgG
IP:CDK8
IB:p65
IB:CDK8
IP:IgG
IP:p65
IB:p65
IB:CDK8
Input
CDK8
p65
β-actin
C
DAPI
CDK8
P65
Merge
NC
IL-1β
10μm
D
Cyto
Nuc
IL-1β
si-hCDK8 #2
si-hNC
p65
β-actin
Histone H3
Cyto
Nuc
IL-1β
OE CDK8
Vector
p65
β-actin
Histone H3
E
Relative luciferace activity of IL-6
pGL3 control
pGL3 IL-6
si-hNC
si-hCDK8 #2
Relative luciferace activity of IL-8
pGL3 control
pGL3 IL-8
si-hNC
si-hCDK8 #2
Relative luciferace activity of MMP13
pGL3 control
pGL3 MMP-13
si-hNC
si-hCDK8 #2
F
Relative luciferace activity of IL-6
Site 4 Site 3 Site 2 Site 1
pGL3 control
-2000
-989
-517
-315
Relative luciferace activity of IL-8
Site 3 Site 2 Site 1
pGL3 control
-2000
-1354
-1021
Relative luciferace activity of MMP-13
Site 3 Site 2 Site 1
pGL3 control
-2000
-1294
-879
G
INPUT
p65 Ab
IgG
OE CDK8
Vector
IL-6
MMP-13
IL-8
H
IL-6
IL-8
MMP-13
Signal relative to input
IgG Ab
P65 Ab
si-hNC
si-hCDK8 #2

maturation and secretion of IL-1β and Caspase-1 (Fig. 6D). In contrast, CDK8 overexpression resulted in the opposite effect (Fig. 6E). ELISA results further demonstrated that the secretion of IL-1β was tightly regulated by CDK8 (Fig. S6E-F). To verify the effect of CDK8 on promoting the inflammatory microenvironment in vivo, we analyzed the performance of CDK8 knockdown and overexpression in mouse synovitis. Consistent with the in vitro results, CDK8 knockdown alleviated the severity of DMM surgery-induced synovitis (Fig. 6F and Fig. S6G), while CDK8 overexpression exacerbated these changes (Fig. 6G and Fig. S6H). The immunohistochemical staining results of synovial tissue further confirmed these effects (Fig. S6I and J). During OA progression, there is bone loss and destruction, a process driven by osteoclasts. To explore whether CDK8 also affects the generation of osteoclasts, we used conditional medium for each group with the same concentrations of M−CSF and RANKL to induce the differentiation of mouse BMDMs into osteoclasts. TRAP staining results showed that CDK8 knockdown inhibited the formation of TRAP-positive multinucleated osteoclasts. The average size of the formed osteoclasts was significantly reduced, and their fusion capacity was impaired (Fig. 6H and I). In contrast, CDK8 overexpression significantly enhanced these parameters (Fig. 6J and K). qPCR analysis of osteoclast differentiation markers also supported these findings (Fig. S6-K-L). To verify whether these effects were consistent in vivo, we performed a comprehensive evaluation using micro-CT and tissue TRAP staining. The micro-CT results further confirmed that inhibiting CDK8 expression alleviated DMM surgery-induced bone destruction (Fig. 6L), while CDK8 overexpression exacerbated these changes (Fig. 6M). Tissue TRAP staining also showed similar results (Fig. S6M). Overall, the results indicate that CDK8 controls the secretion of SASP by chondrocytes, contributing to the formation of an inflammatory microenvironment within the joint, which enhances M1 polarization and inflammasome activation in synovial macrophages, as well as promotes their differentiation into osteoclasts. This series of changes, in turn, accelerates the progression of OA.

CDK8 inhibitors alleviated the progression of OA

To further investigate whether CDK8 inhibitors could be used as a treatment for OA, we selected the CDK8 inhibitor CDK8-IN-6 (Fig. 7A). To study the potential cytotoxicity of CDK8-IN-6, a CCK-8 assay was conducted. At a concentration of 5 μM, no cytotoxic effects were detected in either C28/I2 cells or murine chondrocytes at 24 and 48 h (Fig. 7B). The use of CDK8-IN-6 increased the mRNA and protein levels of aggrecan, COL2A1, and SOX9, which were reduced by IL-1β stimulation, and decreased the elevated levels of MMP-3 and MMP-13 (Fig. 7C-D, and Fig. S7A–C). Similar results were obtained from the IF assay conducted in C28/I2 cells (Fig. 7E). In addition, we observed that CDK8-IN-6 could also inhibit IL-1β-induced phosphorylation of two forms of Rpb1 CTD (Fig. S7D) and affect p65 nuclear translocation in a dose-dependent manner (Fig. S7E). In the results of Safranin O and Toluidine Blue staining, treatment with CDK8-IN-6 reversed the decreased cartilage formation levels in chondrocytes induced by IL-1β stimulation (Fig. 7F, H) and reduced the GAG content resulting from cartilage degradation (Fig. 7G, I).

CDK8-IN-6 selectively inhibits CDK8 to alleviate OA

To understand how CDK8-IN-6 interacts with CDK8, we performed molecular docking simulations. These simulation results revealed nine possible binding sites between CDK8-IN-6 and CDK8, including THR-31, PHE-176, VAL-194/195, PHE-197, ARG-200, LEU-204/205, TYR-211, PRO-246, and HIS-248 (where VAL-194/195 and LEU-204/205 are each considered as a single site) (Fig. 8A). We used DARTS analysis and Western blotting to validate the binding of CDK8-IN-6 to CDK8 and its protection against proteolytic degradation, with the protective effect becoming more pronounced as the concentration of CDK8-IN-6 increased (Fig. 8B). To further investigate the binding mechanism, we mutated these sites to explore which sites have a greater impact on the binding of CDK8-IN-6 to CDK8. According to the results of the DARTS analysis and Western blotting, mutations at all nine sites affected the binding between CDK8-IN-6 and CDK8. However, mutations at the PHE-197, ARG-200, and LEU-204/205 sites had a particularly significant impact on the binding of CDK8-IN-6 to CDK8, almost completely abolishing the protective effect of CDK8-IN-6 against CDK8 proteolysis. This indicates that PHE-197, ARG-200, and LEU-204/205 are crucial for the binding of CDK8-IN-6 to CDK8 (Fig. 8C). To assess CDK8-IN-6′s impact on OA progression in vivo, we administered it twice weekly into the joint cavity of mice, beginning one week post-DMM surgery and continuing until eight weeks post-surgery. Histological analysis showed that the cartilage surface in the DMM group was incomplete with matrix loss. However, treatment with CDK8-IN-6 partially restored cartilage surface integrity and reduced matrix loss (Fig. 8D).The OARSI score indicated that CDK8-IN-6 significantly alleviated the severity of knee joint damage in mice following DMM surgery (Fig. 8E). Immunohistochemical staining demonstrated that intra-articular injection of CDK8-IN-6 enhanced COL2A1 and aggrecan expression and reduced MMP13 levels in mouse cartilage post-DMM surgery (Fig. 8F to I).From the third week onward, the PAM and Von Frey tests indicated a significantly higher pain threshold in the CDK8-IN-6 treatment group compared to the DMM group. This indicates that the use of CDK8-IN-6 not only rescued the cartilage morphology in OA mice but also had a significant alleviated on pain, which is a major clinical symptom of OA (Fig. 8J and Fig. S8).

Discussion

Aside from surgical intervention, effective treatment options for OA are currently unavailable in clinical practice. Improving our understanding of the cellular pathways involved in osteoarthritis

Fig. 4. CDK8 activates the NF-κB pathway and regulates the transcription of SASP. (A) Western blot assay was used to detect the expression levels of p-IκBα, IκBα, p-p65, and p65. (B) Immunoprecipitation was performed to assess the co-precipitation of CDK8 and p65 in C28/I2 cells treated with or without CDK8-IN-6. (C) Immunofluorescence co-localization was conducted to examine the co-localization of p65 and CDK8 in C28/I2 cells treated with IL-1β for 24 h. (D) C28/I2 cells were transfected with si-CDK8 or pCMV3-CDK8, followed by IL-1β treatment for 24 h, and then subjected to western blot analysis of nuclear and cytoplasmic proteins. (E-F) Dual-luciferase analysis demonstrated NF-κB's regulatory role in SASP transcriptional activation (E) and confirmed the direct binding sites of p65 in the promoters of the IL-6, IL-8, and MMP-13 genes (F), the statistical results indicating the significance of the differences between the truncated promoter groups and the full-length group. (G) Nucleic acid electrophoresis and (H) ChIP-qPCR further investigated the influence of CDK8 on the binding of p65 to SASP promoter region sites in C28/I2 cells. (I) Western blot assay was used to detect the expression levels of Rpb1 CTD, p-Rpb1 CTD (Ser2), and p-Rpb1 CTD (Ser5). Data are presented as mean ± SD; *, $p < 0.05$; **, $p < 0.01$; ***, $p < 0.001$; ns, no significance; comparisons with the control group or as indicated.

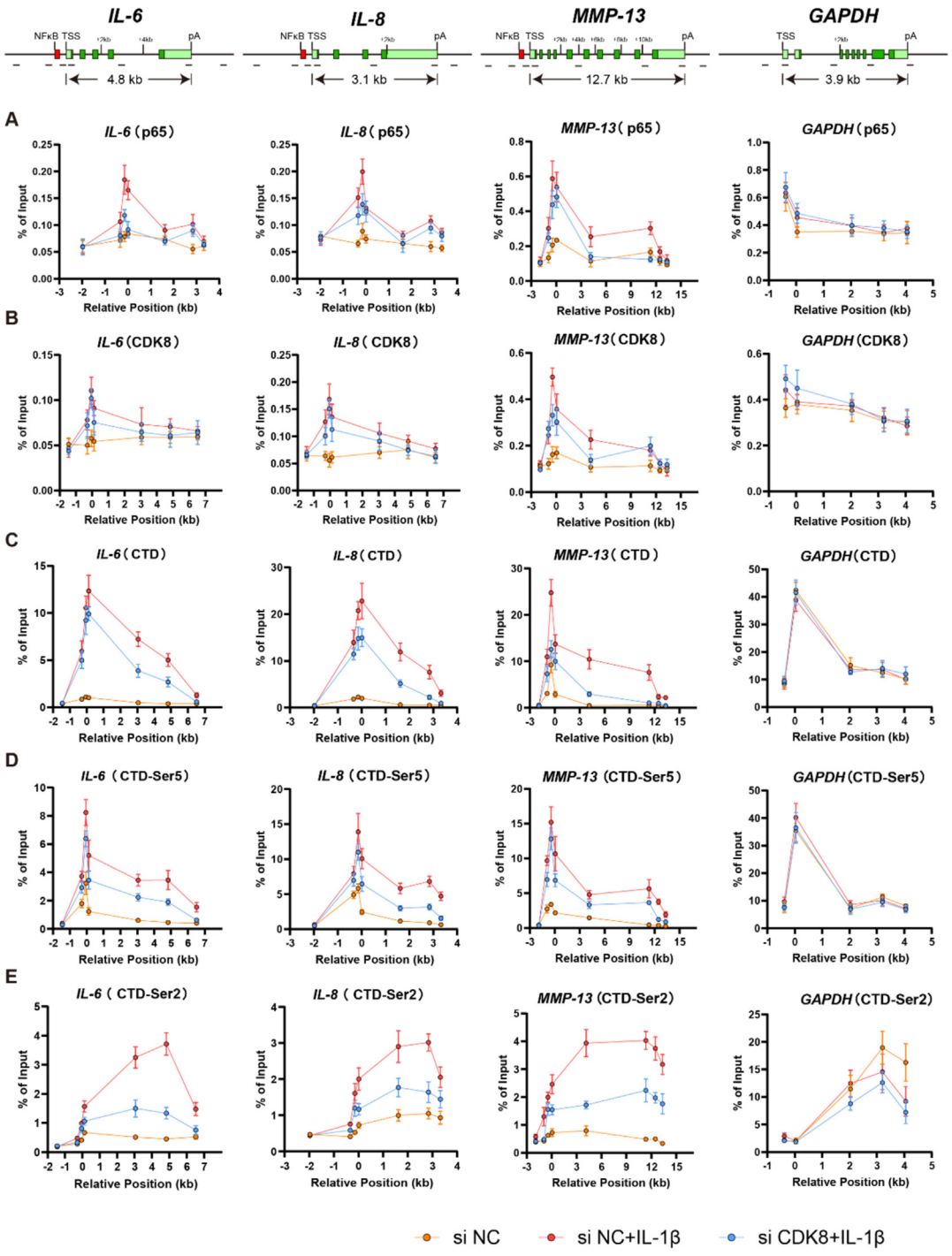

Fig. 5. CDK8 and NF-κB are cooperatively recruited to SASP promoters, leading to elongation phosphorylation of the Rpb1 CTD. In C28/I2 cells transfected with si-NC or si-CDK8, with or without IL-1β treatment for one hour, (A–E) ChIP analysis shows the effects of CDK8 knockdown and IL-1β treatment on the binding of p65 (A), CDK8 (B), Rpb1 CTD (C), Rpb1 CTD phosphorylated at Ser5 (D), and Rpb1 CTD phosphorylated at Ser2 (E) to three SASP genes and a housekeeping gene. The gene diagrams are displayed at the top.

onset and advancement is crucial for enhancing prognosis and creating effective treatments. This study highlights the crucial role of CDK8 in OA progression, investigates the mechanisms of its effect and determines whether CDK8 has potential as a new target for OA treatment. Research has demonstrated that CDK8 is involved in several physiological processes, such as immune response and inflammation [17,34], its effect on OA progression remains unexplored. Our preliminary studies found that overexpression or knockdown of CDK8 in mice and cells correspondingly leads to the exacerbation or alleviation of OA. Our data indicate that inhibiting the expression of CDK8 in chondrocytes under normal conditions does not significantly affect the expression levels of inflammation-related proteins in chondrocytes. This may be because the binding level of CDK8 with NF-κB is relatively low in

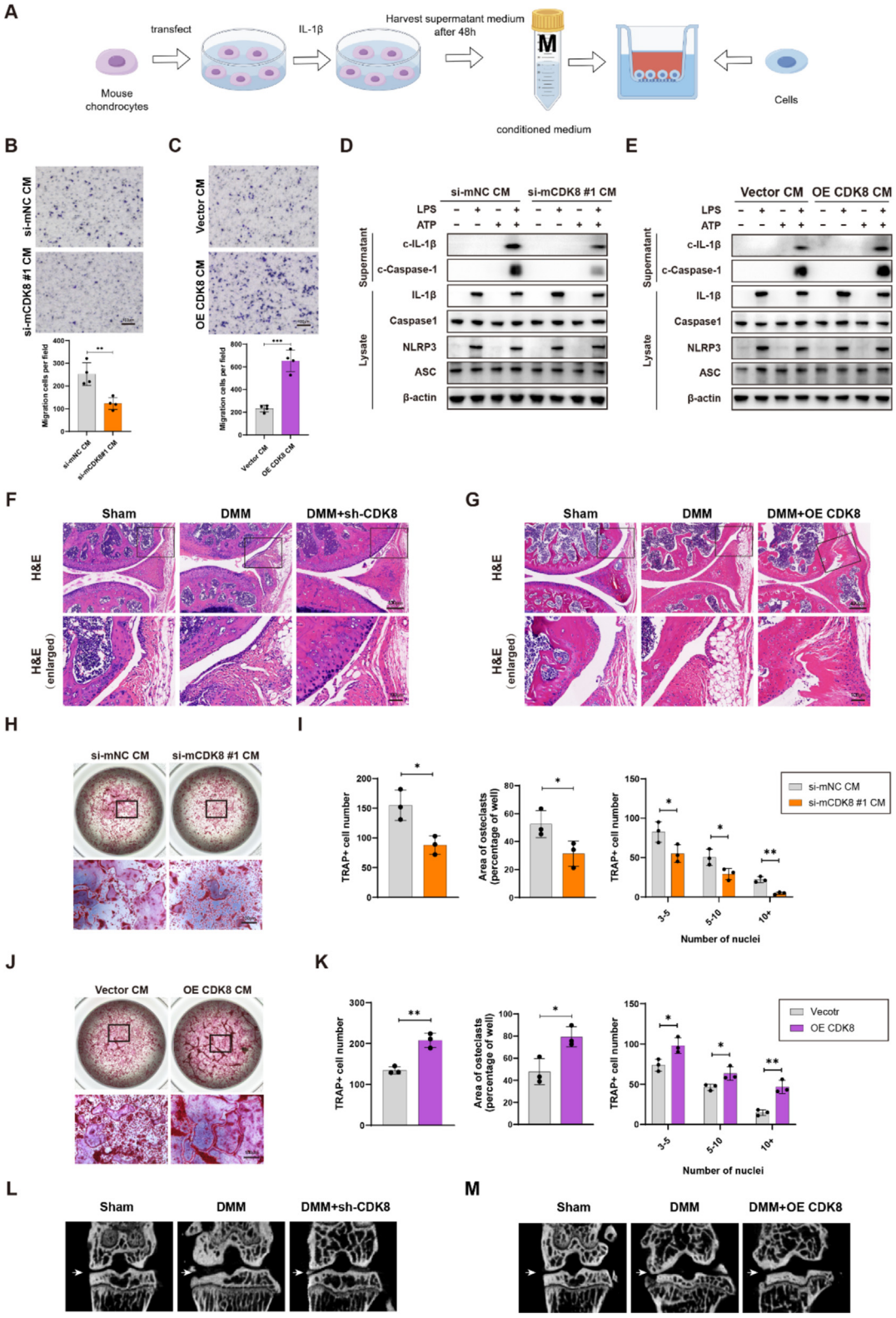

Fig. 6. CDK8 promotes the inflammatory microenvironment and osteoclast differentiation of macrophages by regulating the SASP in chondrocytes. (A) Schematic diagram of the migration assay for RAW 264.7 cells. (B-C) Cell migration ability was evaluated using the migration assay (top) and quantification of migrated cells (bottom). (D-E) Western blotting was used to assess the impact of CDK8 on inflammasome activation in murine synovial macrophages. (F-G) The degree of synovitis was evaluated using H&E-stained sections of mouse knee joints. (H and J) TRAP staining was used to detect the extent of osteoclast differentiation. (I and K) The number and average area of TRAP-positive multinucleated osteoclasts were quantified. The number of TRAP-positive osteoclasts with 3–5, 5–10, or more than 10 nuclei was also determined. (L-M) Bone destruction was assessed by microCT of mouse knee joints, with arrows in the figure indicating the medial side of the knee joints. Data are presented as mean ± SD; *, $p < 0.05$; **, $p < 0.01$; ***, $p < 0.001$; ns, no significance; comparisons with the control group or as indicated.

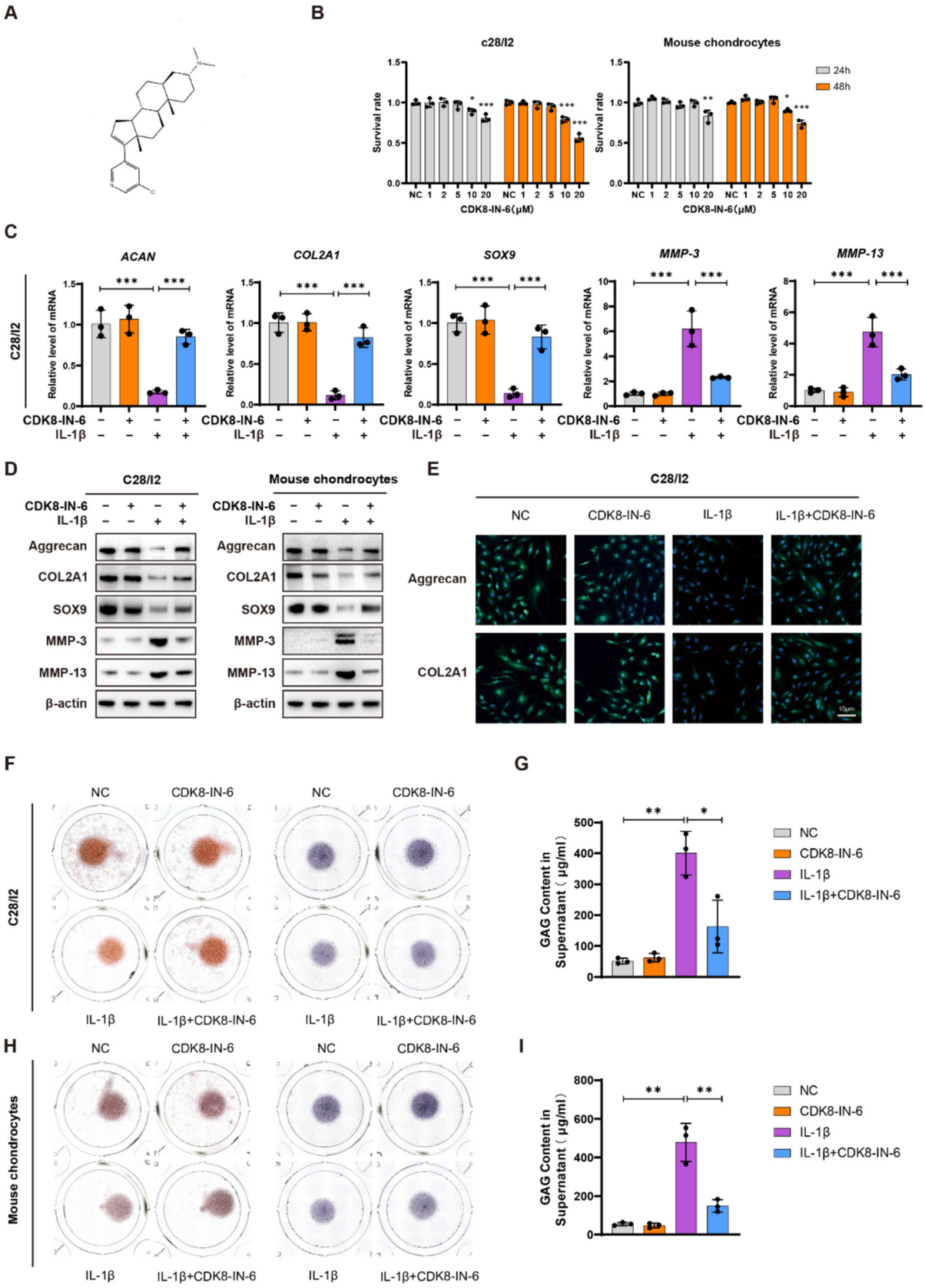

Fig. 7. CDK8 inhibitors alleviated the progression of OA. (A) Molecular structure of CDK8-IN-6. (B) Use the Cell Counting Kit-8 (CCK-8) assay to evaluate the cytotoxic effects of CDK8-IN-6 on C28/I2 cells and mouse chondrocytes at 24 and 48 h. (C-D) C28/I2 cells and mouse chondrocytes were co-treated with IL-1β and CDK8-IN-6 for 48 h. (C) qRT-PCR and (D) Western blot analyses were performed to detect the expression of aggrecan, COL2A1, SOX9, MMP-3, and MMP-13. (E) Immunofluorescence analysis was used to determine the expression of aggrecan and COL2A1 in C28/I2 cells co-treated with IL-1β and CDK8-IN-6 for 48 h. (F, H) Safranin O and Toluidine Blue staining were used to assess cartilage formation in (F) C28/I2 cells and (H) mouse chondrocytes, both treated with IL-1β and CDK8-IN-6 for 7 days. (G, I) The collected supernatants were used to detect GAG content. Data are presented as mean ± SD; *, $p < 0.05$; **, $p < 0.01$; ***, $p < 0.001$; ns, no significance; comparisons with the control group or as indicated. (For interpretation of the references to colour in this figure legend, the reader is referred to the web version of this article.)

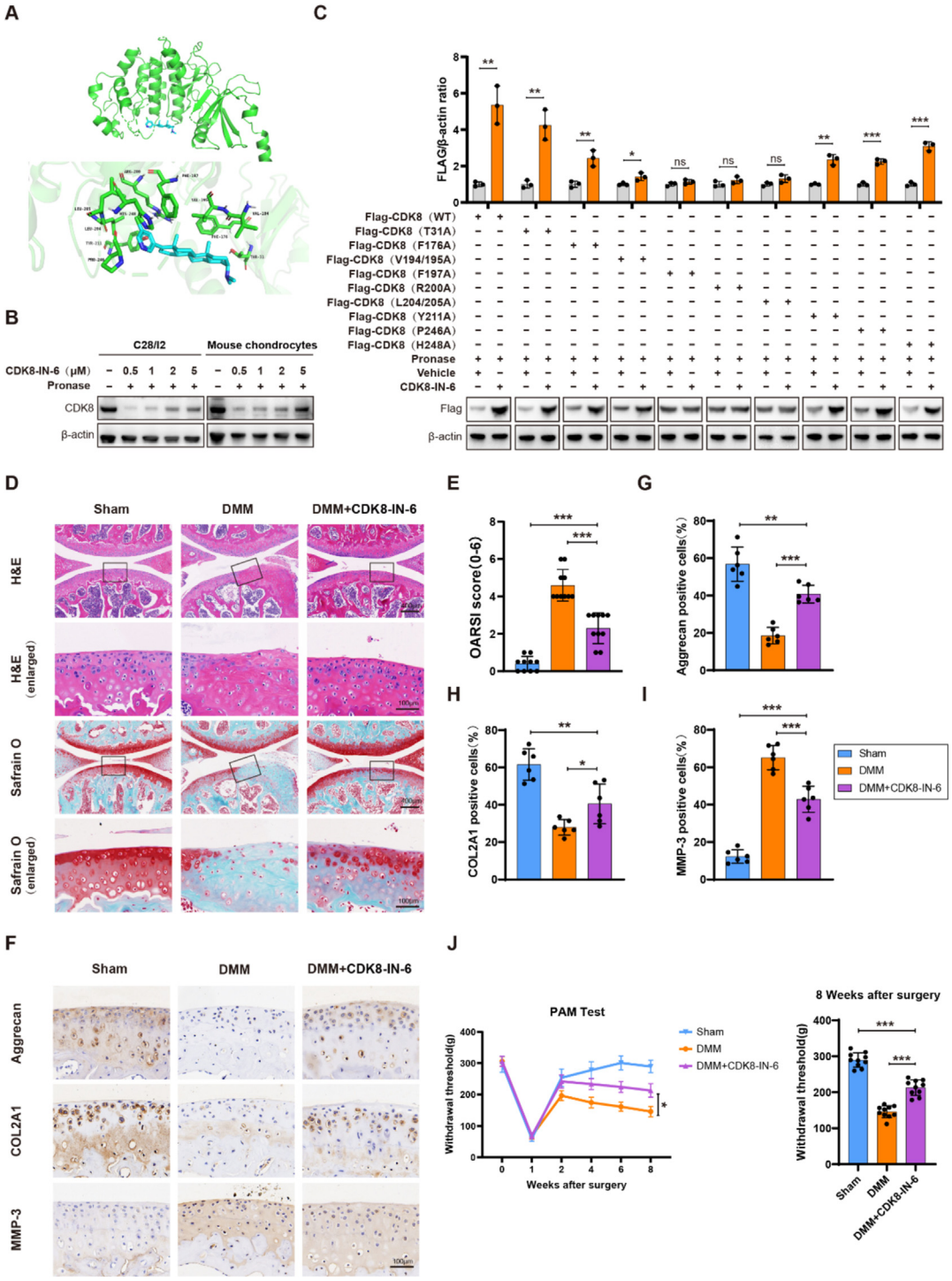

Fig. 8. CDK8-IN-6 selectively inhibits CDK8 to alleviate OA. (A) Docking-predicted binding mode of CDK8 protein with CDK8-IN-6. The overall structure of CDK8 in complex with CDK8-IN-6 in cartoon view. CDK8 and CDK8-IN-6 are colored green and sky blue, respectively (top). Detailed interaction network between CDK8 and CDK8-IN-6, showing all potential binding sites (bottom). (B) Proteins extracted from C28/I2 cells and mouse chondrocytes were used to evaluate the binding of CDK8-IN-6 to CDK8 protein at different concentrations of CDK8-IN-6 and Pronase in DARTS experiments. The binding of CDK8-IN-6 to CDK8 protein was detected by Western blotting. (C) C28/I2 cells were transfected with the indicated CDK8 mutant plasmids for 24 h and subjected to DARTS experiments. Protein expression of the mutated sites was then detected by Western blotting (bottom) and quantified (top). (D) At 8 weeks post-DMM surgery, knee joints from each group of mice were stained with H&E and S-O. (E) Subsequently, the severity of osteoarthritis in mice was assessed using the OARSI scoring system. Each group had n = 10. (F) Expression of Aggrecan, COL2A1, and MMP-3 in cartilage samples was detected by immunohistochemical staining, (G-I) and the proportion of Aggrecan, COL2A1, and MMP-3 positive cells in each section was quantified. Each group had n = 6. (J) Pressure Application Measurement (PAM) test was used to assess the pain threshold in mice. Data are presented as mean ± SD; *, $p < 0.05$; **, $p < 0.01$; ***, $p < 0.001$; ns, no significance; comparisons with the control group or as indicated. (For interpretation of the references to colour in this figure legend, the reader is referred to the web version of this article.)

the absence of inflammatory stimuli. Therefore, under normal physiological conditions, inhibiting the expression of CDK8 may not have a significant effect on alleviating osteoarthritis.

The onset and progression of OA are associated with many physiological and pathological factors [35,36], and during this process, a series of transcriptional and expression changes occur, such

as changes in the expression of inflammatory factors, lipid expression [37], and amino acid expression [38]. According to our RNA sequencing results, CDK8 is closely linked to the NF-κB pathway and cellular senescence. Furthermore, the volcano plot shows that three representative members of the SASP—IL-6, IL-8, and MMP-13—are regulated by CDK8. Cellular senescence plays a important role in the progression of OA. As the progression of OA advances, the number of senescent chondrocytes in the joints continuously increases [39,40]. These senescent chondrocytes exhibit characteristics such as telomere shortening, increased secretion of SASP, elevated production of reactive oxygen species and mitochondrial dysfunction [41–43]. Additionally, intra-articular injection of senescent chondrocytes into mouse joints can induce the formation of OA [44]. Conversely, Intra-articular drug injections targeting senescent cells in cartilage or synovium can markedly decrease SASP secretion and mitigate OA symptoms in mice [45]. Our analysis revealed a notable rise in IL-6, IL-8, and MMP-13 levels in the synovial fluid of OA patients, with this elevation positively correlating with OA severity. The metabolic levels of these three factors in body fluids and cells are also regulated by CDK8, as we verified through detection in mouse body fluids and the supernatant of mouse chondrocytes.

CDK8 is a serine/threonine protein kinase and a member of the CDK family [46,47]. Another member of the CDK family, CDK9, has been shown to have a significant role in regulating transcriptional elongation [18]. This function is primarily achieved through its involvement as part of the P-TEFb (positive transcription elongation factor b) complex, which phosphorylates the CTD of RNA Pol II, thereby promoting transcriptional elongation. Similar to CDK9, CDK8 can also form a kinase module with its corresponding regulatory subunits Cyclin C, MED12, and MED13, acting as part of the mediator complex and playing a crucial role in the transcriptional regulation of RNA Pol II [48–50]. The regulatory role of CDK8 in transcription is likely the mechanism by which CDK8 influences the progression of OA. In previous studies, although CDK8 has been reported to have a regulatory effect on inflammatory factors [17,34] and to interact with NF-κB, influencing its downstream factors [51,52], there is still no definitive conclusion on whether CDK8 affects SASP through its transcriptional regulatory function and the specific mechanisms involved. In this study, we found that in OA, CDK8 influences disease progression by regulating the transcription of the SASP through its interaction with NF-κB. Knocking down CDK8 using siRNA inhibits the transcriptional induction activated by NF-κB. ChIP analysis shows that CDK8 and NF-κB are co-recruited to the promoters of SASP genes. Inhibition of CDK8 kinase affects the binding of p65 to the gene promoter region and slightly affects IL-1β-mediated recruitment of CDK8 to promoters. Crucially, this inhibition reduces the phosphorylation of the C-terminal domain (Rpb1 CTD) of the RNA polymerase II large subunit at the Ser2 and Ser5 sites, thereby impeding the movement of polymerase II along the gene body.CDK8 inhibition specifically affects NF-κB-induced genes without impacting constitutively expressed housekeeping genes. That is, CDK8 interacts with NF-κB to co-recruit to SASP gene promoters, regulating transcription by inducing elongation-specific phosphorylation of the Rpb1 CTD in a gene-specific context.

During the development of OA, in addition to chondrocytes, synovial macrophages also play a critical role as key regulators in the physiological and pathological processes [53], maintaining an active state in OA joints. Increasing evidence indicates that imbalanced M1/M2 synovial macrophages are closely linked to synovial inflammation, cartilage damage, and OA severity. We utilized conditioned medium (CM) prepared from the culture medium of mouse chondrocytes to culture mouse synovial macrophages, aiming to explore the crosstalk between chondrocytes and synovial macrophages during the OA process. We found that CM prepared from chondrocytes with high CDK8 expression drove synovial macrophages towards M1 polarization and promoted inflammasome activation in these macrophages. This process leads to the maturation and secretion of the inflammatory factors IL-1β and Caspase-1, further promoting the formation of an inflammatory microenvironment within the joint, inducing chondrocytes to secrete more SASP. At the same time, synovial macrophages are also driven toward osteoclast differentiation, resulting in bone loss and destruction. These processes together cause the progression of OA to fall into a vicious cycle.

We also used the CDK8 inhibitor CDK8-IN-6 to further investigate whether CDK8 inhibitors could be used as a drug for OA treatment. Through various in vitro and in vivo methods, including cell studies, micromass culture, and mouse models, we demonstrated that CDK8 inhibitors can slow the progression of OA. Using methods such as molecular docking simulations and DARTS, we confirmed the binding of CDK8-IN-6 to the CDK8 protein and identified their main binding sites. In summary, our research demonstrates that the mechanism by which CDK8 influences the progression of OA is through its interaction with NF-κB to regulate the transcription of SASP, while also promoting M1 polarization of synovial macrophages and inflammasome activation in these macrophages, thereby affecting the development of osteoarthritis.

However, this study still has several limitations that need to be further addressed in future research. Firstly, the study findings are primarily based on preclinical models (e.g., mouse models and in vitro systems). While these models provide critical evidence for elucidating the functions and mechanisms of CDK8, they may not fully capture the complex pathology of human OA. For example, there are certain differences between the joint structures and inflammatory responses of mice and humans, which may limit the translational potential of the study findings to clinical applications. Therefore, further validation of CDK8′s role in large animal models and human samples is needed, particularly in terms of its specific effects under physiological and pathological conditions of the joint. In addition, we did not delve into the off-target effects or potential toxicity of CDK8 inhibitors. Although CDK8-IN-6 demonstrated the potential to slow OA progression in our study, CDK8, as a serine/threonine protein kinase, may have other undefined roles in different cells and tissues. Consequently, CDK8 inhibitors may induce nonspecific effects, leading to off-target effects or toxicity. For example, CDK8′s broad roles in immune regulation and metabolic pathways could disrupt systemic immune balance or metabolic homeostasis. Future research should focus on systematically evaluating the safety and toxicity of CDK8 inhibitors, particularly regarding potential adverse effects from long-term treatment.Additionally, this study primarily relied on CDK8 knockdown and inhibitors without explicitly investigating whether CDK8 modulation might trigger unintended systemic effects. For instance, CDK8′s impact on RNA Pol II transcription regulation could interfere with the expression of normal genes, potentially leading to unexpected systemic side effects. Although our data suggest that CDK8 primarily affects NF-κB-induced gene expression without disrupting essential housekeeping genes, this conclusion requires validation in broader in vivo systems. Future studies could leverage gene-editing technologies, such as CRISPR/Cas9, to further evaluate the systemic regulatory role of CDK8 and its potential nonspecific effects. Long-term treatment experiments should also be designed to assess the impact of CDK8 inhibitors on multiple tissues and systems, especially regarding potential toxicity in the skeletal, immune, and cardiovascular systems. Additionally, studies should investigate the efficacy and safety of CDK8 inhibitors under different doses and administration routes to optimize therapeutic strategies. In future research, we also plan to explore the role of CDK8 in other joint tissues, such as synovium and bone. This study primarily focused on the function of CDK8 in chondrocytes,

but synovium and bone tissues also play significant roles in the onset and progression of OA. How CDK8 contributes to OA pathology through its effects on synovial cell proliferation and inflammatory responses or its regulation of bone remodeling processes (e.g., osteoclast differentiation) remains to be further explored. Future studies could use tissue-specific CDK8 knockout mouse models (e.g., cartilage-specific or synovium-specific knockout models) to address these questions.

In summary, this study provides preliminary scientific evidence for CDK8 as a therapeutic target for OA. However, multiple issues remain to be resolved before its clinical application, including validation in different OA models, exploration of its role in other joint tissues, and systematic studies on the long-term safety and efficacy of CDK8 inhibitors. We believe that with further research into CDK8 functions and the mechanisms of its inhibitors, this target has the potential to play an important role in future OA therapies.

Conclusion

During the progression of OA, the SASP secreted by chondrocytes is an important factor in exacerbating OA. This study reveals that CDK8 regulates the transcriptional levels of SASP by being cooperatively recruited with NF-κB to the promoters of SASP genes, and subsequently promoting elongation phosphorylation of Rpb1 CTD in the NF-κB-induced gene-specific context. Inhibiting CDK8 expression can reduce the secretion of SASP and alleviate the inflammatory microenvironment resulting from its secretion. Therefore, targeting CDK8 inhibition could serve as a promising approach for OA treatment.

CRediT authorship contribution statement

Zhongnan Lin: Conceptualization, Methodology, Writing – original draft. **Yining Xu:** Software, Methodology. **Hongyi Jiang:** Methodology. **Wen Zeng:** Software, Formal analysis. **Yuhan Wang:** Data curation. **Liang Zhu:** Data curation. **Chihao Lin:** Formal analysis. **Chao Lou:** Data curation. **Hanting Shen:** Methodology, Data curation. **Han Ye:** Software. **Yean Gu:** Software. **Huachen Yu:** Funding acquisition. **Xiaoyun Pan:** Conceptualization, Funding acquisition, Writing – review & editing. **Lin Zheng:** Conceptualization, Funding acquisition, Writing – review & editing.

Declaration of competing interest

The authors declare that they have no known competing financial interests or personal relationships that could have appeared to influence the work reported in this paper.

Acknowledgement

This work was supported by grants from the National Natural Science Foundation of China (grant number: 82302749), the Basic Research Funds Project of Wenzhou Medical University, China (grant number: KYYW202304), and the Wenzhou Municipal Basic Research Project (grant number: 2024Y0551). The schematic diagrams of the migration assay and the majoy molecular pathways were drawn by Figdraw.

Appendix A. Supplementary data

Supplementary data to this article can be found online at https://doi.org/10.1016/j.jare.2025.01.017.

References

[1] Neogi T. The epidemiology and impact of pain in osteoarthritis. Osteoarthritis Cartilage 2013;21(9):1145–53.
[2] Cai J, Liu LF, Qin Z, Liu S, Wang Y, Chen Z, et al. Natural Morin-Based Metal Organic Framework Nanoenzymes Modulate Articular Cavity Microenvironment to Alleviate Osteoarthritis. Research (Wash D C) 2023;6:0068.
[3] Robinson WH, Lepus CM, Wang Q, Raghu H, Mao R, Lindstrom TM, et al. Low-grade inflammation as a key mediator of the pathogenesis of osteoarthritis. Nat Rev Rheumatol 2016;12(10):580–92.
[4] Choi WS, Lee G, Song WH, Koh JT, Yang J, Kwak JS, et al. The CH25H-CYP7B1-RORα axis of cholesterol metabolism regulates osteoarthritis. Nature 2019;566 (7743):254–8.
[5] Yang G, Wang Y, Zeng Y, Gao GF, Liang X, Zhou M, et al. Rapid health transition in China, 1990–2010: findings from the Global Burden of Disease Study 2010. Lancet 2013;381(9882):1987–2015.
[6] Kloppenburg M, Berenbaum F. Osteoarthritis year in review 2019: epidemiology and therapy. Osteoarthritis Cartilage 2020;28(3):242–8.
[7] Yang J, Wang X, Fan Y, Song X, Wu J, Fu Z, et al. Tropoelastin improves adhesion and migration of intra-articular injected infrapatellar fat pad MSCs and reduces osteoarthritis progression. Bioact Mater 2022;10:443–59.
[8] Lv Z, Wang P, Li W, Xie Y, Sun W, Jin X, et al. Bifunctional TRPV1 Targeted Magnetothermal Switch to Attenuate Osteoarthritis Progression. Research (Wash D C) 2024;7:0316.
[9] Wei H, Huang H, He H, Xiao Y, Chun L, Jin Z, et al. Pt-Se Hybrid Nanozymes with Potent Catalytic Activities to Scavenge ROS/RONS and Regulate Macrophage Polarization for Osteoarthritis Therapy. Research (Wash D C) 2024;7:0310.
[10] López-Otín C, Blasco MA, Partridge L, Serrano M, Kroemer G. The hallmarks of aging. Cell 2013;153(6):1194–217.
[11] Coryell PR, Diekman BO, Loeser RF. Mechanisms and therapeutic implications of cellular senescence in osteoarthritis. Nat Rev Rheumatol 2021;17(1):47–57.
[12] Faust HJ, Zhang H, Han J, Wolf MT, Jeon OH, Sadtler K, et al. IL-17 and immunologically induced senescence regulate response to injury in osteoarthritis. J Clin Invest 2020;130(10):5493–507.
[13] Kang C, Xu Q, Martin TD, Li MZ, Demaria M, Aron L, et al. The DNA damage response induces inflammation and senescence by inhibiting autophagy of GATA4. Science 2015;349(6255):aaa5612.
[14] Xu C, Tang Y, Yang H, Jiang S, Peng W, Xie R. Harpagide inhibits the TNF-α-induced inflammatory response in rat articular chondrocytes by the glycolytic pathways for alleviating osteoarthritis. Int Immunopharmacol 2024;127:111406.
[15] de Andrés MC, Takahashi A, Oreffo RO. Demethylation of an NF-κB enhancer element orchestrates iNOS induction in osteoarthritis and is associated with altered chondrocyte cell cycle. Osteoarthritis Cartilage 2016;24(11):1951–60.
[16] Haudenschild DR, Carlson AK, Zignego DL, Yik JHN, Hilmer JK, June RK. Inhibition of early response genes prevents changes in global joint metabolomic profiles in mouse post-traumatic osteoarthritis. Osteoarthritis Cartilage 2019;27(3):504–12.
[17] Johannessen L, Sundberg TB, O'Connell DJ, Kolde R, Berstler J, Billings KJ, et al. Small-molecule studies identify CDK8 as a regulator of IL-10 in myeloid cells. Nat Chem Biol 2017;13(10):1102–8.
[18] Zhang H, Pandey S, Travers M, Sun H, Morton G, Madzo J, et al. Targeting CDK9 Reactivates Epigenetically Silenced Genes in Cancer. Cell 2018;175(5):1244.
[19] Bourbon HM. Comparative genomics supports a deep evolutionary origin for the large, four-module transcriptional mediator complex. Nucleic Acids Res 2008;36(12):3993–4008.
[20] Li J, Xu P, Wu D, Guan M, Weng X, Lu Y, et al. Hypoxic stress suppresses lung tumor-secreted exosomal miR101 to activate macrophages and induce inflammation. Cell Death Dis 2021;12(8):776.
[21] Moyo MB, Parker JB, Chakravarti D. Altered chromatin landscape and enhancer engagement underlie transcriptional dysregulation in MED12 mutant uterine leiomyomas. Nat Commun 2020;11(1):1019.
[22] Bardeck N, Paluschinski M, Castoldi M, Kordes C, Görg B, Stindt J, et al. Swelling-induced upregulation of miR-141-3p inhibits hepatocyte proliferation. JHEP Rep 2022;4(4):100440.
[23] Glasson SS, Chambers MG, Van Den Berg WB, Little CB. The OARSI histopathology initiative - recommendations for histological assessments of osteoarthritis in the mouse. Osteoarthritis Cartilage 2010;18(Suppl 3):S17–23.
[24] Zhang H, Lin C, Zeng C, Wang Z, Wang H, Lu J, et al. Synovial macrophage M1 polarisation exacerbates experimental osteoarthritis partially through R-spondin-2. Ann Rheum Dis 2018;77(10):1524–34.
[25] Kuang L, Wu J, Su N, Qi H, Chen H, Zhou S, et al. FGFR3 deficiency enhances CXCL12-dependent chemotaxis of macrophages via upregulating CXCR7 and aggravates joint destruction in mice. Ann Rheum Dis 2020;79(1):112–22.
[26] Guo S, Ernstsen C, Hay-Schmidt A, Kristensen DM, Ashina M, Olesen J, et al. PACAP signaling is not involved in GTN- and levcromakalim-induced hypersensitivity in mouse models of migraine. J Headache Pain 2022;23 (1):155.
[27] Eldridge SE, Barawi A, Wang H, Roelofs AJ, Kaneva M, Guan Z, et al. Agrin induces long-term osteochondral regeneration by supporting repair morphogenesis. Sci Transl Med 2020;12(559).
[28] Wu Y, Shen S, Chen J, Ni W, Wang Q, Zhou H, et al. Metabolite asymmetric dimethylarginine (ADMA) functions as a destabilization enhancer of SOX9 mediated by DDAH1 in osteoarthritis. Sci Adv 2023;9(6):eade5584.

[29] Clements KM, Flannelly JK, Tart J, Brockbank SM, Wardale J, Freeth J, et al. Matrix metalloproteinase 17 is necessary for cartilage aggrecan degradation in an inflammatory environment. Ann Rheum Dis 2011;70(4):683–9.
[30] Asfaha S, Dubeykovskiy AN, Tomita H, Yang X, Stokes S, Shibata W, et al. Mice that express human interleukin-8 have increased mobilization of immature myeloid cells, which exacerbates inflammation and accelerates colon carcinogenesis. Gastroenterology 2013;144(1):155–66.
[31] Yu W, Xie Z, Li J, Lin J, Su Z, Che Y, et al. Super enhancers targeting ZBTB16 in osteogenesis protect against osteoporosis. Bone Res 2023;11(1):30.
[32] Gold MO, Tassan JP, Nigg EA, Rice AP, Herrmann CH. Viral transactivators E1A and VP16 interact with a large complex that is associated with CTD kinase activity and contains CDK8. Nucleic Acids Res 1996;24(19):3771–7.
[33] Culemann S, Grüneboom A, Nicolás-Ávila J, Weidner D, Lämmle KF, Rothe T, et al. Locally renewing resident synovial macrophages provide a protective barrier for the joint. Nature 2019;572(7771):670–5.
[34] Malumbres M. Cyclin-dependent kinases. Genome Biol 2014;15(6):122.
[35] Timmins KA, Leech RD, Batt ME, Edwards KL. Running and Knee Osteoarthritis: A Systematic Review and Meta-analysis. Am J Sports Med 2017;45(6):1447–57.
[36] Mandl LA. Osteoarthritis year in review 2018: clinical. Osteoarthritis Cartilage 2019;27(3):359–64.
[37] Loef M, Ioan-Facsinay A, Mook-Kanamori DO, Willems van Dijk K, de Mutsert R, Kloppenburg M, et al. The association of plasma fatty acids with hand and knee osteoarthritis: the NEO study. Osteoarthritis Cartilage 2020;28(2):223–30.
[38] Piepoli T, Mennuni L, Zerbi S, Lanza M, Rovati LC, Caselli G. Glutamate signaling in chondrocytes and the potential involvement of NMDA receptors in cell proliferation and inflammatory gene expression. Osteoarthritis Cartilage 2009;17(8):1076–83.
[39] Wakale S, Wu X, Sonar Y, Sun A, Fan X, Crawford R, et al. How are Aging and Osteoarthritis Related? Aging Dis 2023;14(3):592–604.
[40] Diekman BO, Sessions GA, Collins JA, Knecht AK, Strum SL, Mitin NK, et al. Expression of p16(INK)(4a) is a biomarker of chondrocyte aging but does not cause osteoarthritis. Aging Cell 2018;17(4):e12771.
[41] Di Micco R, Krizhanovsky V, Baker D, d'Adda di Fagagna F. Cellular senescence in ageing: from mechanisms to therapeutic opportunities. Nat Rev Mol Cell Biol 2021;22(2):75–95.
[42] Jeon OH, David N, Campisi J, Elisseeff JH. Senescent cells and osteoarthritis: a painful connection. J Clin Invest 2018;128(4):1229–37.
[43] Loeser RF. Aging and osteoarthritis: the role of chondrocyte senescence and aging changes in the cartilage matrix. Osteoarthritis Cartilage 2009;17(8):971–9.
[44] Xu M, Bradley EW, Weivoda MM, Hwang SM, Pirtskhalava T, Decklever T, et al. Transplanted Senescent Cells Induce an Osteoarthritis-Like Condition in Mice. J Gerontol A Biol Sci Med Sci 2017;72(6):780–5.
[45] Childs BG, Gluscevic M, Baker DJ, Laberge RM, Marquess D, Dananberg J, et al. Senescent cells: an emerging target for diseases of ageing. Nat Rev Drug Discov 2017;16(10):718–35.
[46] Nemet J, Jelicic B, Rubelj I, Sopta M. The two faces of Cdk8, a positive/negative regulator of transcription. Biochimie 2014;97:22–7.
[47] Conaway RC, Sato S, Tomomori-Sato C, Yao T, Conaway JW. The mammalian Mediator complex and its role in transcriptional regulation. Trends Biochem Sci 2005;30(5):250–5.
[48] Tsai KL, Sato S, Tomomori-Sato C, Conaway RC, Conaway JW, Asturias FJ. A conserved Mediator-CDK8 kinase module association regulates Mediator-RNA polymerase II interaction. Nat Struct Mol Biol 2013;20(5):611–9.
[49] Yan YY, Zhang XX, Xiao Y, Shen XB, Jian YJ, Wang YM, et al. Design and Synthesis of a 2-Amino-pyridine Derivative as a Potent CDK8 Inhibitor for Anti-colorectal Cancer Therapy. J Med Chem 2022;65(19):13216–39.
[50] Poss ZC, Ebmeier CC, Odell AT, Tangpeerachaikul A, Lee T, Pelish HE, et al. Identification of Mediator Kinase Substrates in Human Cells using Cortistatin A and Quantitative Phosphoproteomics. Cell Rep 2016;15(2):436–50.
[51] Chen M, Li J, Zhang L, Wang L, Cheng C, Ji H, et al. CDK8 and CDK19: positive regulators of signal-induced transcription and negative regulators of Mediator complex proteins. Nucleic Acids Res 2023;51(14):7288–313.
[52] Chen M, Liang J, Ji H, Yang Z, Altilia S, Hu B, et al. CDK8/19 Mediator kinases potentiate induction of transcription by NFκB. Proc Natl Acad Sci U S A 2017;114(38):10208–13.
[53] Kraus VB, McDaniel G, Huebner JL, Stabler TV, Pieper CF, Shipes SW, et al. Direct in vivo evidence of activated macrophages in human osteoarthritis. Osteoarthritis Cartilage 2016;24(9):1613–21.